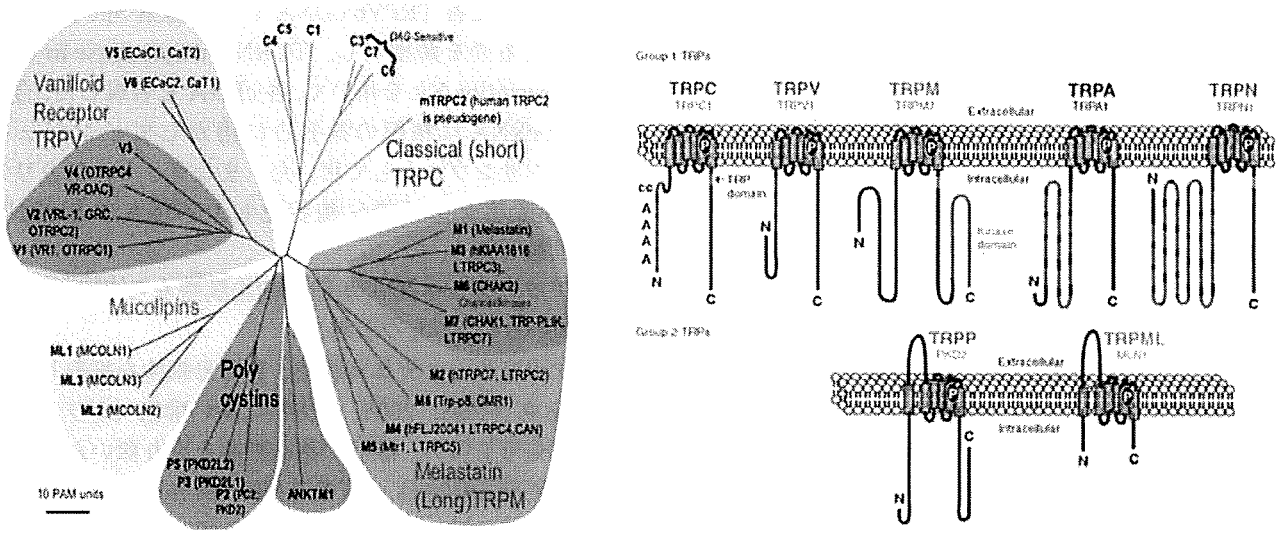

図1　TRPチャネルファミリーの分類

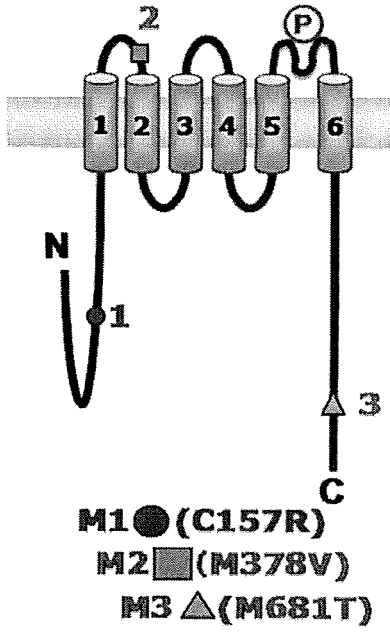

図2　獲得型TRPV6アミノ酸変異

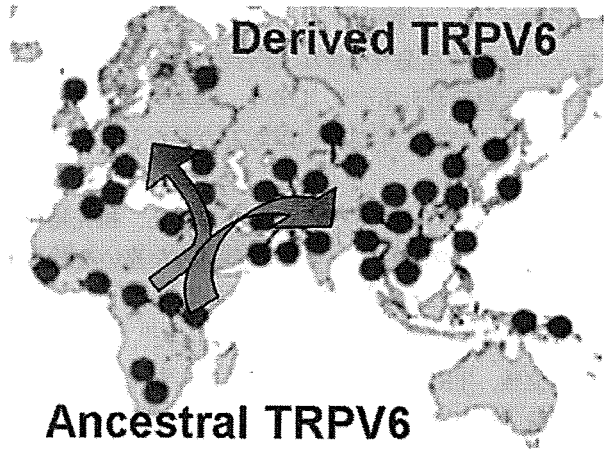

図3　祖先型（Ancestral）と獲得型（Derived）TRPV6の分布

哺乳類では構造の違いから6～7つのサブファミリーに分かれており，近年急速に研究が進展してきたチャネルファミリーである．

今回解析を行ったTRPV6は，はじめCAT1やECaC2と呼ばれていたが，のちにカプサイシンレセプターで知られるTRPV1と同じバニロイドチャネルファミリーに属していることがわかった．しかしTRPV1～4とは異なり，温度依存性やプロトン感受性はなく，Ca^{2+}を選択的に透過するチャネルであることが特徴的である．TRPV6チャネルは特に小腸（粘膜上皮細胞）において特異的発現が見られ，食物からのカルシウム吸収ならびに生体でのカルシウム濃度調節に重要な働きを担っている[1,2]．これまでの報告ではビタミンD3によってTRPV6蛋白の発現が誘導されること，PKC（プロテインキナーゼC）によるリン酸化を受けることがわかっており，近年では，前立腺におけるTRPV6の過剰発現と前立腺がんとの関与が示唆されている．

2006年5月，TRPV6には2つのタイプが存在することが報告された．アフリカを起源とするタイプ（祖先型TRPV6）と，3塩基変異を獲得したタイプ（獲得型TRPV6：祖先型TRPV6からC157R，M378V，

M681Tの箇所のアミノ酸が変異したもの：図2）があり，獲得型TRPV6はアフリカから急速に全世界に広がり，現在大半を占めるTRPV6遺伝型となっている[3]．

図3で調べられているのはアフリカ，アジア，ヨーロッパにおけるそれぞれのTRPV6の分布であるが，アフリカを起源とする祖先型と，アフリカ以外の地域で見られる3塩基変異型の獲得型が存在し，ヨーロッパ・アジア地域では獲得型が広く分布している[3]．

遺伝子配列の解析により，獲得型TRPV6はわずか6000～7000年という短い期間で，アジアやヨーロッパに広まったことが判明した[3]．通常，遺伝子変異は10万年から100万年の歳月をかけて起こると考えられているのに対し，獲得型TRPV6は非常に短い期間で変異を遂げている．これはTRPV6遺伝子にポジティブセレクションが行われたことを示唆し，獲得型TRPV6には，人類がアフリカ以外のアジア・ヨーロッパ地域で生息するのに都合の良い機能や条件があったと想像される[3)~5)]．しかし，両者のTRPV6チャネル機能にどのような違いがあるのかなど，その詳細は不明である．

今回，このバックグラウンドをふまえ，祖先型ならびに獲得型TRPV6チャネルの機能的な違いを検討するために，それぞれのTRPV6チャネルクローンを発現させ，機能評価を行う方法を確立した[6]．機能評価法の確立後，TRPV6クローンをアフリカツメガエル卵母細胞，BHK細胞に発現させ，様々な解析を行った．

実験方法

cDNAならびにcRNA作製

合成プライマーを用いて，白人由来のヒト胎盤cDNAライブラリー（Clontech）よりTRPV6領域全長をPCRにて増幅した．PCRは，98℃30秒で変性，98℃7秒の変性，68℃30秒のアニーリング，72℃75秒の伸長反応の条件で35サイクルの反応を行った．その後PCR産物をpGEM-He-Juel及びpcDNA3.1（－）ベクターに挿入し，これらを獲得型TRPV6の組み換えクローンとして用いた．祖先型TRPV6の組み換えクローンは，獲得型TRPV6を鋳型にして，QuikChange Multi Site-Directed Mutagenesis Kit（Stratagene）を用いて変異体として作製した．変異を起こした配列はシークエンスにより確かめ，pGEM-He-Juel及びpcDNA3.1（－）ベクターを用いて祖先型TRPV6組み替えクローンを作製した．pGEM-He-Juelベクターに組み替えた各TRPV6 cDNAを制限酵素Spe Iで線状化したものを鋳型にし，T7 RNA polymerase in vitro transcription Kitを用いて，各cRNAを合成した．合成したcRNAは精製の後H_2Oに溶かしてインジェクションサンプルとして用いた．またラットムスカリン性M_1受容体も同様に線状化したcDNAよりcRNAを作製した．

アフリカツメガエル卵母細胞調整ならびにTRPV6 cRNAのインジェクション

アフリカツメガエル腹腔より卵母細胞を採取し，Uezonoら（1993，2006）の方法に従い酵素（コラゲネース）処理を行い，膜状の濾胞細胞を取り除いた[6)7)]．調整した卵母細胞は，ND96 buffer（96 mM NaCl，2 mM KCl，1.8 mM $CaCl_2$，1 mM $MgCl_2$，5 mM HEPES，pH 7.4）に，2.5 mMのピルビン酸ナトリウムと，50 mg/mlのゲンタマイシンを含む溶液を用いて18℃で培養した．cRNA溶液は，TRPV6 cRNA 5 ngとラットムスカリンM_1受容体cRNA 1 ngの比率で注入されるように調整し，それらを卵母細胞に注入し，TRPV6チャネルならびにM_1受容体を発現させた．その後電気生理学アッセイを行うまで3～8日間，ND96 bufferを用いて18℃で培養した．

電気生理学的アッセイ

Geneclamp 500 amplifierアッセイ装置を用いて卵母細胞膜を二極電極で電位固定し，刺激により流れる電流を室温にて測定した．卵母細胞は－60mVに固定し，Ca^{2+}-freeのND-96 bufferを5 ml/minの流量で流し，Ca^{2+}-freeより1.8 mM Ca^{2+}濃度のND-96に変換することにより流れる電流を測定した[5)6)10)]．0.6～2.0 MΩの抵抗を持つ電極を3M KClで満たし，測定に使用した．測定データはMacLab（AD Instruments）を用いて連続的に記録した．またM_1受容体アゴニストであるアセチルコリン（3×10^{-7}M）をCa^{2+}-freeのND-96 bufferで溶解し使用した．

Baby hamster kidney（BHK）cellの培養ならびにcDNAトランスフェクション

BHK細胞は，95%air/5%CO_2含有インキュベーターにて37℃で培養した．35 mmのグラスボトムディッシュに1×10^5個の細胞をまいた．Uezono（2006）及びKanaide（2007）らの方法に従い，非リポソーム脂質系脂質のEffecteneトランスフェクション試薬（Qiagen）を用いて，各TRPV6 in pcDNA3.1（－）cDNAを0.2 μgずつトランスフェクションした[8)9)]．トランスフェクション後16～24時間後の細胞を解析に用いた．トラン

スフェクション効率は24時間後でおよそ70%であった.

細胞内 Ca^{2+} 濃度インジケーター G-CaMP2-NT を発現させた BHK 細胞を用いてのカルシウムイメージング

細胞膜直下のカルシウム濃度変化を可視化できるカルシウムインジケーター蛍光蛋白 pN1-G-CaMP2-NT cDNA[13][14]を，それぞれのTRPV6 cDNAとともにBHK細胞に共発現させた．細胞外溶液を Ca^{2+}-free の ND-96 から 18 mM の ND-96 に置換し，変化する蛍光を共焦点レーザー顕微鏡（LSM510 META）でモニタリングした．蛍光観察は 488 nm レーザー光を当て，510 nm にて緑色に光る蛍光の強さを測定した．

TRPV6 の細胞内局在

終止コドンを除いたTRPV6の全長コード領域のC末端に，蛍光蛋白をコードするCerulean及びVenusのcDNAを連結させ，pcDNA3.1(−)ベクターに組み込んだ発現クローンを作製した．発現クローンをそれぞれBHK細胞にトランスフェクションし，共焦点レーザーを用いて458 nmの波長を当てた．TRPV6-Ceruleanは480 nmの青い蛍光を[11]，TRPV6-Venusは530 nmの黄色い蛍光を[12]発する．黄色，青色に光っている部位を解析することで，BHK細胞におけるそれぞれのTRPV6の発現部位とした[8][9]．

Fluorescence resonance energy transfer（FRET）assay

35 mmのグラスボトムディッシュに培養したBHK細胞に，CeruleanまたはVenusを融合させた祖先型及び獲得型TRPV6を0.2 μgずつ共発現させた．共焦点レーザーのFRETアッセイシステムを用いてTRPV6-Cerulean及びTRPV6-Venusの蛋白質複合体の形成度合いを分析した[8][9]．Uezono(2006)およびKanaide(2007)らの報告にあるように，458 nmの波長により蛍光を発するCeruleanはVenusが近接していれば蛍光を転移する性質があるため，Venusの蛍光を退色させることによって転移していたCerulean蛍光を回復させるアクセプターブリーチング法を利用し，FRETの有無を検討した．FRETが起こっている場合は，Cerulean（青色）の増加率をもとにFRET効率を算出した．

Western blot 法

祖先型及び獲得型TRPV6 cRNAをそれぞれインジェクションしたアフリカツメガエル卵母細胞を超音波処理後，蛋白を可溶化した．可溶化抽出溶液を遠心（15,000 rpm×30 min）した後，上清をウェスタンブロット分析用のサンプルとして−80℃に保存した．

0.1Mの2-メルカプトエタノールを含むLaemmeli sample bufferとサンプルを混合させたものを95℃ 5分間反応させ，その後10%SDS-ポリアクリルアミドゲル電気泳動を行い，PVDFメンブレンに転写し，TRPV6の抗ヤギポリクローナル抗体を用いて免疫ブロットを行った．

TRPV6蛋白の発現を確認するためのポリクローナル抗体はSanta Cruz Biotechnology社，N末端マッピングTRPV6（N-16）抗体を使用した．

続く2次抗体はホースラディッシュペルオキシダーゼで標識したヤギ抗IgG抗体を使用した．各抗体は1次抗体を1：200，2次抗体を1：1,000の割合で溶解したものを使用した．検出には，Chemiluminescence Western blot detection reagents（Nacalai Tesque）を用いた．

結　果

アフリカツメガエル卵母細胞に発現させた TRPV6 チャネル機能の電気生理的アッセイ

祖先型TRPV6チャネルとムスカリニック M_1R とを共発現させたアフリカツメガエル卵母細胞を用いて，細胞外 Ca^{2+} の濃度を0 mMから1.8 mMに置換したときに流れる電流を測定したところ，内向きカレントが見られた．TRPV6チャネルを発現させていない卵母細胞ではカレントは全く見られなかった（data not shown）．TRPV6チャネルを発現させた卵母細胞でみられたカレントは解析の結果，卵母細胞に内在性に存在している Ca^{2+}-activated Cl^- チャネルからの Cl^- カレントであり，TRPV6チャネルより外液 Ca^{2+} が流入し，その結果 Ca^{2+}-activated Cl^- カレントが引き起こされたものと考えられた．同様の検討を獲得型TRPV6についても行った．

図4A，Bに示すように，M_1R を発現させた卵母細胞では，アセチルコリンにより細胞内 Ca^{2+} が上昇し，その結果 Ca^{2+}-activated Cl^- カレントが流れる[10]．このカレントを測定することにより，卵母細胞におけるTRPV6/M_1R cRNAインジェクション後のTRPV6と M_1R との発現程度を確認した．発現が同程度である，つまり M_1R による Cl^- カレントがほぼ同じ大きさの卵母細胞を用いてTRPV6によるカレントを比較した．

各々の卵母細胞による発現の個体差をなくすため，TRPV6によるカレント値を M_1R によるカレント値で

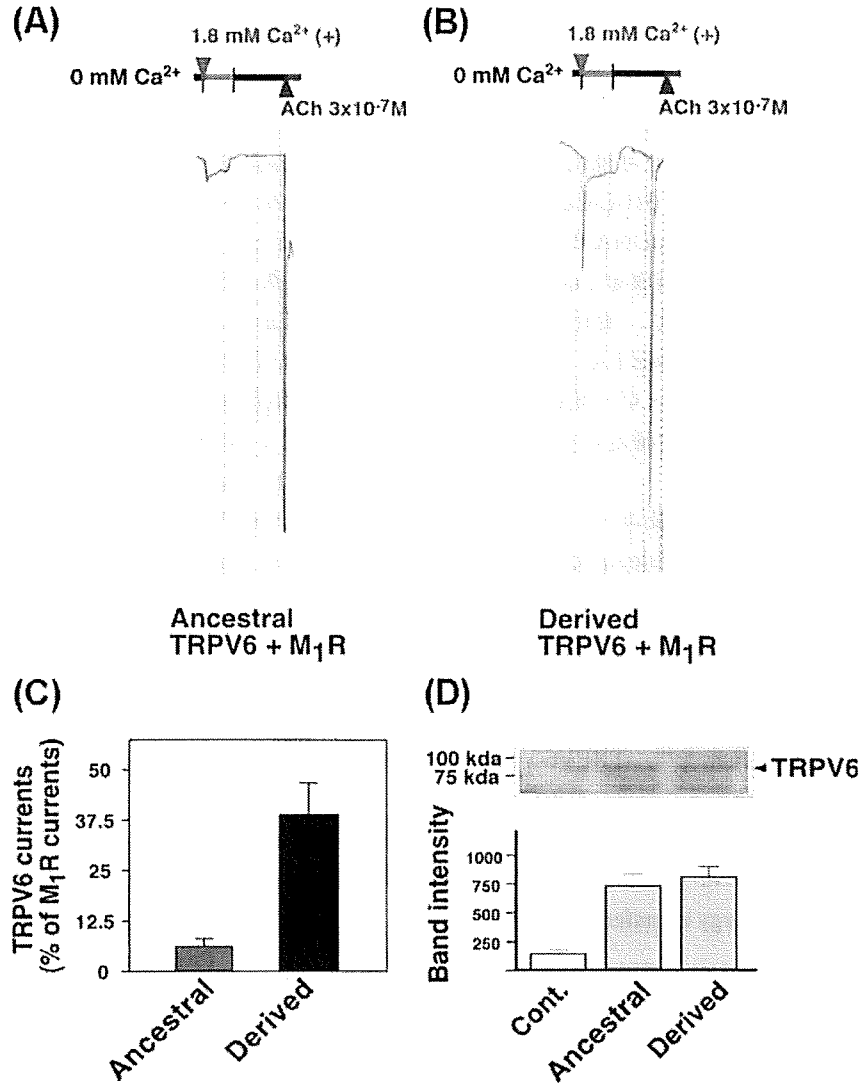

図4　細胞外液カルシウム濃度を0 mMから1.8 mMへ上げた際の Ca^{2+}-activated Cl^- channelの活性化．TRPV6チャネルを発現させた*Xenopus* oocytesを用いて，(A) 祖先型（Ancestral）および (B) 獲得型（Derived）TRPV6チャネル活性化による細胞内カルシウム上昇に伴う典型的な Ca^{2+}-activated Cl^- channelからの Cl^- カレント，並びに 3×10^{-7}M アセチルコリンによるムスカリン性受容体（M_1R）活性化による Cl^- カレント．(C) M_1R 活性化による Cl^- カレントと，TRPV6チャネル活性化による Cl^- カレントの比．（各々 n = 10）．(D)ウェスタンブロットによるTRPV6チャネル蛋白発現の比較．Cont. TRPV6 cRNAをインジェクションしていない卵母細胞からのサンプル，Ancestral. 祖先型TRPV6 cRNAをインジェクションしたもの，Derived. 獲得型TRPV6 cRNAをインジェクションさせたもの．Band intensity，デンシトメーターでそれぞれのバンドを計測した値．（各々 n = 4）．

割った相対値で表し，祖先型TRPV6，ならびに獲得型TRPV6チャネル機能を比較した．獲得型TRPV6のカレントは祖先型に比べ大きく，すなわち獲得型TRPV6は祖先型に比べて多くの細胞外カルシウムを取り込むことが示唆された（図4C）．

Western blot法によるツメガエル卵母細胞でのTRPV6蛋白発現量の確認

電気生理学的アッセイを行った後の卵母細胞より蛋白抽出を行い，ウェスタンブロット法でTRPV6チャネル蛋白の検出を試みたところ，祖先型及び獲得型

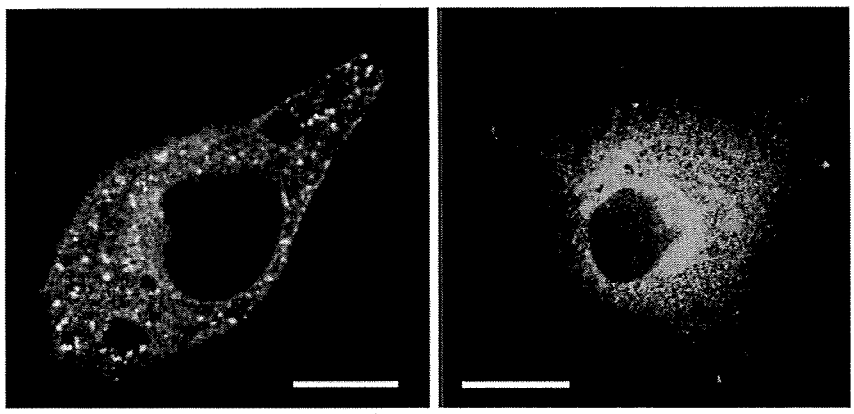

図5 共焦点レーザ顕微鏡による祖先型TRPV6-Venusと獲得型TRPV6-Ceruleanの像
Bar = 20μm

TRPV6では，両者ともにTRPV6を示す80～85 kDa付近のバンドが検出され，その発現量に違いは見られなかった(図4D)．つまり，TRPV6によるカレントの大きさの違いは，チャネル蛋白発現量に由来するものではなく，チャネル活性自体に違いがあると考えられた．

G-CaMP2-NTを用いてのカルシウムイメージング—TRPV6発現細胞を用いての検討—

祖先型ならびに獲得型TRPV6と，細胞内Ca^{2+}濃度上昇に伴い緑の蛍光を増強させる蛍光蛋白G-CaMP2-NTを同時にBHK cellにトランスフェクションした．外液のCa^{2+}濃度を0 mMから18 mMに上昇させると，細胞外Ca^{2+}がTRPV6を介して流入し，上昇した細胞内Ca^{2+}はG-CaMP2-NTの緑色蛍光を増強させた(Fig. 2A left)．TRPV6のみを発現させていた細胞では，0 mMから18 mMにCa^{2+}を上昇させても蛍光の増強は得られなかった（data not shown)．

蛍光変化のタイムコースを数個の細胞のCa^{2+}上昇の結果から計算すると，緑色蛍光，すなわちカルシウム濃度は急速に上昇し，その後，元のレベルまで戻ることがわかった．祖先型と獲得型のTRPV6でのCa^{2+}上昇の度合いを比較すると，Ca^{2+}を添加した後の蛍光変化のタイムコースは祖先型，獲得型ともほぼ同様で，蛍光の一過性増強が観察されたが，獲得型TRPV6の蛍光は，祖先型と比較し，著明な蛍光の増強を示した(data not shown)．

TRPV6蛋白の細胞内局在及び多量体化についての検討

蛍光蛋白で標識したTRPV6-Venus及びTRPV6-CeruleanをBHK細胞に発現させ，共焦点レーザーを用いてTRPV6の細胞内局在を観察した．黄色に光るTRPV6-Venus，青色に光るTRPV6-Ceruleanはともに細胞質，及び細胞膜上に全体的に発現していた(図5)．

FRETアッセイならびにアクセプターブリーチング法にて，TRPV6が多量体を形成しているか否かを解析した．祖先型TRPV6-Venusと祖先型TRPV6-Ceruleanを同時に発現させたBHK細胞においては，図5のように，蛍光は細胞膜，細胞質に全体的に発現していた．祖先型TRPV6-Cerulean/Venusを共発現させたBHK細胞を用いて細胞膜でのアクセプターブリーチングを行ったところ，Venusの蛍光強度の減少に伴いCeruleanの蛍光増強が観察された．アクセプターブリーチング法で，Venusの蛍光強度を減少させたときに同時にCeruleanの蛍光増加がみられれば，これは蛋白同士，この場合はそれぞれのTRPV6チャネルが近接化していることを示す．すなわち，祖先型TRPV6-CeruleanとTRPV6-Venusは蛋白複合体を形成していること，おそらくホモテトラマーを形成していると考えられた．同様に，獲得型TRPV6-Crulean/Venusについても行ったところ，同じくホモテトラマー蛋白複合体の形成が確認された（data not shown)．

ポジティブコントロールとして，蛋白同士の複合体形成が確かめられている$GABA_{B1}$受容体-Venusと$GABA_{B2}$受容体-Ceruleanを共発現させた細胞においてアクセプターブリーチングを行ったデータと比較したところ，祖先型及び獲得型のFRET効率の値は，$GABA_B$受容体の効率とほぼ同等であり，祖先型TRPV6と獲得型TRPV6も同程度に多量体（4量体）を形成することが推測された（data not shown)．

考 察

TRPV6は，主に小腸に発現し，カルシウムを選択的に透過するチャネルであり[1)2)]，食物からのカルシウム吸収に重要な働きを担っている[1)2)]．このTRPV6にはアフリカを起源とする祖先型と，アフリカ以外のヨーロッパ・アジア地域等で見られる3塩基変異を持つ獲得型があり，世界中に広く分布している[3)]．

遺伝子配列の解析により，獲得型TRPV6はわずか7000年という短い期間で，アジアやヨーロッパに広まったことが判明した[3)]．これはTRPV6遺伝子にポジティブセレクションが行われ，獲得型TRPV6には，人類がアフリカの以外のアジア・ヨーロッパ地域で生息するのに都合の良い機能や条件があったと想像されている[3)]．しかしそれらチャネル機能の違い等については不明であった．

私たちは2つの発現系を用いてTRPV6チャネル機能，ならび細胞内でのTRPV6チャネル発現様式を解析した．その結果，獲得型のTRPV6チャネルは祖先型TRPV6チャネルに対し高いカルシウム透過性を示すこと，すなわち獲得型TRPV6チャネルと祖先型TRPV6チャネルではチャネル機能に違いがあることを見出した．

高いCa^{2+}透過性を持つ獲得型TRPV6チャネルを持つ人種がなぜヨーロッパ・アジアなどに急速に広がり，しかも祖先型TRPV6チャネルを持つアフリカ地域には獲得型TRPV6を持つ人が少ないのか，現在のところ不明である．

Akey(2006)らは，アフリカ以外の人類ではTRPV6チャネルに何らかの機能，あるいは選択の利点があって獲得型TRPV6を持つ人々が増えてきたのだろうと推測している[3)]．獲得型TRPV6は免疫学的にT細胞の活性化に優位であろう，あるいはある種の感染に強いのではといった推測を彼らは行っているが，それは推測の域を出ず，実際に獲得型TRPV6の何が優位であるのか示されていない[3)]．

今回の研究で私たちは，獲得型TRPV6が祖先型TRPV6に比べCa^{2+}透過性が高い事を示した．TRPV6蛋白はVitamin D3や紫外線によって発現誘導されることが知られている[15)]．つまり多量のVitamin D3，多くの紫外線によりTRPV6蛋白発現は増加する[1)2)]．従って，自然選択が行われた時期の環境背景（今から7000年前は氷河期が終了し，地球が徐々に回復している時期であった．この当時アフリカ以外の地域は紫外線量が優位に低い）をふまえると，アジア・ヨーロッパの地域においては，アフリカほど紫外線が強くないためにTRPV6蛋白発現の誘導がかかりにくかったことが想像される．そのため蛋白自身の発現が少なくても，獲得型TRPV6のようにそれ自身で高いCa^{2+}透過性を持ち，発現量を補うことのできるチャネルが選択されてきたのではないかと推察される．つまり高いCa^{2+}透過性を示す獲得型TRPV6を持つ人類が優位に生き残り，そして繁栄して行ったのではないかと想像される．今後はこの獲得型TRPV6の高いCa^{2+}透過性を示す責任遺伝子の特定など，獲得型TRPV6チャネルと祖先型TRPV6チャネルの特性の比較を分子生物学的，電気生理学的，組織学的に詳しく解析していきたい．さらに，TRPV6チャネルの基礎情報を蓄積することで，関与する疾病の発症メカニズムや人種差による違い，加えて治療に向けての可能性を期待できるのではないかと考えている．

終わりに

私たちは，獲得型ならびに祖先型TRPV6のCa^{2+}透過性に違いがあることを見出した．この結果をふまえ，獲得型TRPV6のポジティブセレクションにいたる紫外線の影響の関与を提唱した．獲得型TRPV6の自然選択が行われた当時は氷河期が終わった直後の気候回復期に当たり，アフリカ以外のヨーロッパ・アジア地域では紫外線が強くなかったと推測されている．その条件下では，TRPV6蛋白の発現誘導はかかりにくいと考えられる．おそらく，少ないTRPV6発現量を補うことのできる高いCa^{2+}透過性の「獲得型TRPV6」を持った人類が生態系に都合の良い結果として優位に生き残り，繁栄したのではないかと考えられた．

§文 献

1) van Abel M, Hoenderop JG, Bindels RJ. The epithelial calcium channels TRPV5 and TRPV6: regulation and implications for disease. Naunyn Schmiedeberg's Arch Pharmacol 2005; 371: 295—306.
2) Nijenhuis T, Hoenderop JG, Bindels RJ. TRPV5 and TRPV6 in Ca^{2+} (re) absorption: regulating Ca^{2+} entry at the gate. Pflugers Arch 2005; 451: 181—192.
3) Akey JM, Swanson WJ, Madeoy J, et al. TRPV6 exhibits unusual patterns of polymorphism and divergence in worldwide populations. Hum Mol Genet 2006; 15: 2106—2113.

4) Soejima M, Tachida H, Ishida T, et al. Evidence for recent positive selection at the human AIM1 locus in a European population. Mol Biol Evol 2006; 23: 179—188.
5) Akey JM, Eberle MA, Rieder MJ, et al. Population history and natural selection shape patterns of genetic variation in 132 genes. PLoS Biol 2004; 2: e 286.
6) Uezono Y, Bradley J, Min C, et al. Receptors that couple to 2 classes of G proteins increase cAMP and activate CFTR expressed in *Xenopus* oocytes. Receptors Channels 1993; 1: 233—241.
7) Uezono Y, Akihara M, Kaibara M, et al. Activation of inwardly rectifying K^+ channels by GABA-B receptors expressed in *Xenopus* oocytes. Neuroreport 1998; 9: 583—587.
8) Uezono Y, Kanaide M, Kaibara M, et al. Coupling of $GABA_B$ receptor $GABA_{B2}$ subunit to G proteins: evidence from *Xenopus* oocyte and baby hamster kidney cell expression system. Am J Physiol Cell Physiol 2006; 290: C200—207.
9) Kanaide M, Uezono Y, Matsumoto M, et al. Desensitization of $GABA_B$ receptor signaling by formation of protein complexes of $GABA_{B2}$ subunit with GRK4 or GRK5. J Cell Physiol 2007; 210: 237—245.
10) Minami K, Vanderah TW, Minami M, et al. Inhibitory effects of anesthetics and ethanol on muscarinic receptors expressed in *Xenopus* oocytes. Eur J Pharmacol 1997; 339: 237—244.
11) Rizzo MA, Piston DW. High-contrast imaging of fluorescent protein FRET by fluorescence polarization microscopy. Biophys J 2005; 88: L14—16.
12) Nagai T, Ibata K, Park ES, et al. A variant of yellow fluorescent protein with fast and efficient maturation for cell-biological applications. Nat Biotechnol 2002; 20: 87—90.
13) Ohkura M, Matsuzaki M, Kasai H, et al. Genetically encoded bright Ca^{2+} probe applicable for dynamic Ca^{2+} imaging of dendritic spines. Anal Chem 2005; 77: 5861—5869.
14) Nakai J, Ohkura M, Imoto K. A high signal-to-noise Ca^{2+} probe composed of a single green fluorescent protein. Nat Biotechnol 2001; 19: 137—141.
15) Hoenderop JG, Voets T, Hoefs S, et al. Homo- and heterotetrameric architecture of the epithelial Ca^{2+} channels TRPV5 and TRPV6. EMBO J 2003; 22: 776—785.

Neuroscience Letters 451 (2009) 270–273

Contents lists available at ScienceDirect

Neuroscience Letters

journal homepage: www.elsevier.com/locate/neulet

Cell-dependent physiological synaptic action of morphine in the rat habenular nucleus: Morphine both inhibits and facilitates excitatory synaptic transmission

Keisuke Hashimoto[a], Taku Amano[a,b], Norio Sakai[b], Tsutomu Suzuki[a,**], Minoru Narita[a,*]

[a] Department of Toxicology, Hoshi University School of Pharmacy and Pharmaceutical Sciences, 2-4-41 Ebara, Shinagawa-ku, Tokyo 142-8501, Japan
[b] Department of Molecular and Pharmacological Neuroscience, Division of Integrated Medical Science, Graduate School of Biomedical Sciences, Hiroshima University, 1-2-3 Kasumi, Minami-ku, Hiroshima 734-8551, Japan

ARTICLE INFO

Article history:
Received 3 December 2008
Received in revised form
26 December 2008
Accepted 7 January 2009

Keywords:
Morphine
Opioid
Thalamus
Habenular nucleus
mEPSC

ABSTRACT

Although several lines of evidence have suggested that the activity of thalamic neurons is modulated by opioids, the mechanism by which morphine in the thalamus regulates the release of excitatory neurotransmitters remains unclear. In the present study, we investigated the synaptic modulation of morphine to regulate excitatory synaptic transmission, probably glutamatergic transmission, in habenular nucleus (Hb) and centrolateral nucleus (CL) neurons in the rat thalamus. Using the whole-cell patch-clamp technique, we found dual modulation by morphine in Hb neurons: morphine caused either inhibition or facilitation of the miniature excitatory postsynaptic current (mEPSC) frequency in the Hb. In Hb neurons that showed a morphine-induced decrease in the mEPSC frequency, the mEPSC amplitude was also decreased in the presence of morphine. In contrast, the mEPSC amplitude was markedly increased in Hb neurons that showed a morphine-induced increase in the mEPSC frequency. We also observed a significant decrease in the mEPSC frequency with morphine in CL neurons without any change in the mEPSC amplitude, whereas morphine did not facilitate the mEPSC frequency in CL neurons. These results suggest that morphine may induce cell-dependent dual modulation of glutamatergic synaptic transmission in the Hb.

There is broad agreement on the general outlines of the afferent transmission pathways from primary afferent nociceptors through the spinal dorsal horn to the thalamus. Indeed, noxious stimulation activates thalamic neurons including the centrolateral nucleus (CL) in the medial thalamus and the habenular nucleus (Hb) in the epithalamus, as revealed by electrophysiological studies [1,8,26,27,31,32]. Studies on the supraspinal projection of spinothalamic pathways have suggested that the medial thalamus including the CL relays peripheral nociceptive information to the frontal part of the cortex and plays an important role in the affective and motivational aspects of pain processing [3,11,37]. In contrast, the Hb receives input from the limbic forebrain and pallidum and, in turn, projects to numerous midbrain structures [12,13]. Previous works have shown that analgesia could be achieved by electrical or chemical stimulation of the Hb [5,6,19,33,34]. These results suggest that a potential antinociceptive effect may originate via the Hb.

Autoradiographic, mRNA and immunohistochemical studies have shown the localization of μ-opioid receptors (MORs) in the thalamus, including the Hb and the CL [21–23]. Stimulation of MORs by the MOR-selective agonist D-Ala^2, N-MePhe^4, Gli-ol^5-enkephalin (DAMGO) results in an increase of an inwardly rectifying potassium conductance, which hyperpolarizes the cell and changes its firing pattern on the postsynaptic membrane in the CL [2]. Our previous study showed that stimulation of MOR by morphine in the Hb may be involved in activation of a descending antinociceptive pathway via excitatory synaptic transmission [28]. Although these results have suggested that the activity of thalamic neurons may be either positively or negatively modulated by morphine, the effect of morphine in thalamic transmission remains unclear. Therefore, the present study was undertaken to investigate the role of morphine in the presynaptic modulation of excitatory synaptic transmission in rat Hb and CL neurons. We observed the dual modulation of excitatory synaptic transmission by morphine in Hb neurons: morphine in the rat Hb caused either inhibition or facilitation of the miniature excitatory postsynaptic current (mEPSC) frequency. In contrast, morphine only produced a reduction of the mEPSC frequency in CL neurons.

The present study was conducted in accordance with the Guiding Principles for the Care and Use of Laboratory Animals (Hoshi University), as adopted by the Committee on Animal Research of Hoshi University, which is accredited by the Ministry of Education, Culture, Sports, Science, and Technology of Japan.

After young Sprague Dawley rats (10–18 days old) were decapitated, a block of tissue containing the thalamus was trimmed.

* Corresponding author. Tel.: +81 3 5498 5628; fax: +81 3 5498 5628.
** Co-corresponding author. Tel.: +81 3 5498 5831; fax: +81 3 5498 5831.
E-mail addresses: suzuki@hoshi.ac.jp (T. Suzuki), narita@hoshi.ac.jp (M. Narita).

0304-3940/$ – see front matter © 2009 Elsevier Ireland Ltd. All rights reserved.
doi:10.1016/j.neulet.2009.01.009

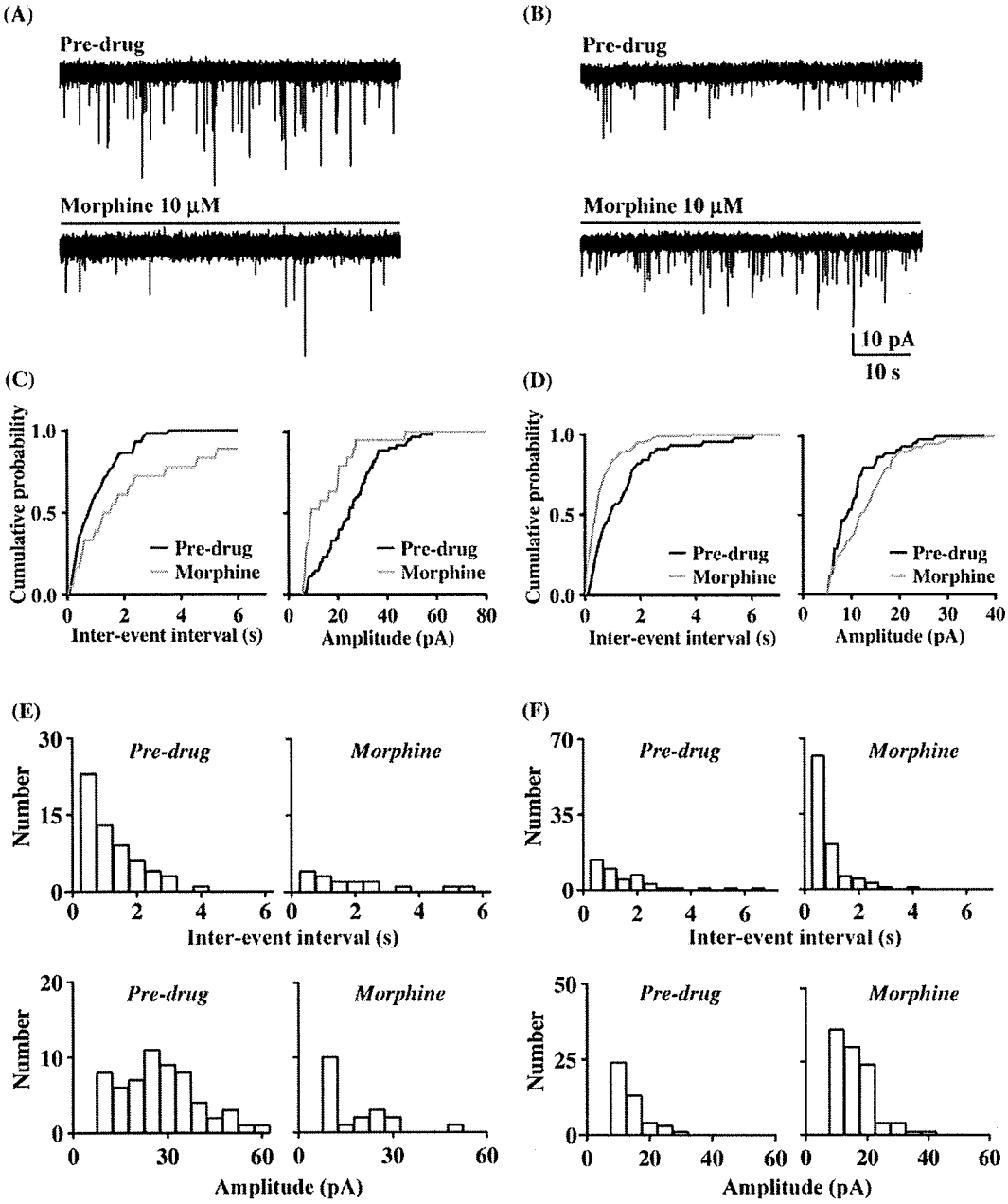

Fig. 1. Presynaptic effects of morphine in the habenular nucleus (Hb). (A and B) Representative mEPSCs recorded in the absence (pre-drug; top) or presence of 10 μM morphine (bottom) at a holding potential of −70 mV. Bath application of morphine for 3 min induced a marked decrease (A) or increase (B) in the mEPSC amplitude and frequency in Hb neurons. (C and D) Cumulative distributions of the mEPSC inter-event interval or amplitude obtained from the same neuron as shown in (A) or (B), respectively, in the absence (pre-drug) or presence of morphine. (E and F) Histograms of the number of events per minute plotted against the inter-event interval (top) or amplitude (bottom) in the absence (pre-drug; left) or presence of morphine (right). Data were obtained from the same neuron as shown in (A) or (B), respectively.

Thalamic coronal slices (150 μm thick) were cut from the block using a microslicer (DTK-1000; Dosaka, Kyoto, Japan) and perfused at a rate of 3 ml/min with artificial cerebrospinal fluid (in mM: NaCl 117, KCl 3.6, $CaCl_2$ 2.5, $MgCl_2$ 1.2, NaH_2PO_4 1.2, $NaHCO_3$ 25 and glucose 11) along with the sodium channel blocker tetrodotoxin (TTX) 0.3 μM (Wako Chemicals, Osaka, Japan), which was saturated with 5% CO_2 and 95% O_2 at room temperature. Standard whole-cell voltage-clamp recordings were made from thalamic neurons using an EPC8 amplifier (Heka, Lambrecht, Germany). Neurons were visualized under Nomarski optics with a water-immersion lens (BX-50WI; Olympus, Tokyo, Japan). The microelectrode solution had the following composition (in mM): potassium gluconate 136, KCl 5, $CaCl_2$ 0.5, $MgCl_2$ 2, EGTA 5, HEPES 5 and MgATP 5. The patch microelectrodes were made from borosilicate capillary glass and had resistances of 5–10 MΩ for the whole-cell recording. Under voltage-clamp recording conditions, the series resistance was 4–7 MΩ. The signals filtered at 3 kHz were directly digitized and stored on a personal computer. These sampled measurements were analyzed using the pCLAMP8 program (Axon Instruments). Miniature excitatory postsynaptic currents were analyzed using the MiniAnalysis Program (Synaptosoft Inc., Decatur, GA, USA).

Whole-cell patch-clamp recordings were performed in Hb neurons of P10-18 thalamic slices. In the voltage-clamp mode, mEPSCs were observed in 17 Hb neurons and 11 CL neurons at a hold-

ing potential of −70 mV. In the present study, these mEPSCs were completely blocked by 10 μM CNQX and 10 μM MK-801 (data not shown), indicating that they were mediated by glutamate receptors. We first investigated whether morphine changes the properties of mEPSCs in the Hb. Bath application of morphine induced a marked decrease ($n = 6$, Fig. 1A, C and E) or increase ($n = 5$, Fig. 1B, D and F) in the mEPSC amplitude and frequency in Hb neurons. The morphine-induced decrease or increase in mEPSC frequency was observed in approximately 35% or 30% of Hb neurons that showed mEPSCs, respectively. The average decrease or increase in the mEPSC number per minute was 58.4 ± 11.6% or 191.5 ± 48.1% of the control, respectively ($p < 0.05$, Student's t-test). In Hb neurons that showed a morphine-induced decrease in the mEPSC frequency, the mEPSC amplitude was also decreased in the presence of morphine (4 of 6 neurons) (Fig. 1C and E). The average decrease in the mEPSC amplitude per minute was 69.8 ± 6.0% of the control ($n = 4$, $p < 0.05$, Student's t-test). Interestingly, the mEPSC amplitude was markedly increased in Hb neurons that showed a morphine-induced increase in the mEPSC frequency (2 of 5 neurons, Fig. 1 D and F). In the remaining neurons tested (6 of 17 neurons), bath application of morphine failed to change the mEPSC frequency.

We next investigated whether morphine affected the properties of mEPSCs in the CL. The application of morphine reduced the mEPSC frequency in CL neurons (Fig. 2A). This morphine-induced decrease in the mEPSC frequency was observed in approximately 35% of the CL neurons examined (4 of 11 neurons). The average decrease in the mEPSC frequency was 60.2 ± 5.9% of the control ($n = 4$, $p < 0.05$, Student's t-test). Application of morphine prolonged the inter-event interval of the mEPSC frequency without affecting its amplitude in CL neurons (Fig. 2B and C). In the remaining CL neurons tested (7 of 11 neurons), the bath application of morphine did not change the mEPSC frequency. Morphine did not facilitate the mEPSC frequency in CL neurons.

It has been reported that MOR agonists presynaptically inhibit glutamatergic synaptic transmission in the spinal dorsal horn [15–17], midbrain periaqueductal gray (PAG) [36] and cultured hippocampal neurons [18]. In the present study, morphine decreased the frequency of mEPSC that was blocked by CNQX and MK-801 in both Hb and CL neurons. The frequency of mEPSCs depends on the probability of neurotransmitter release from presynaptic terminals [10]. The present data suggest that morphine may act presynaptically to inhibit glutamate release in the Hb and CL.

The CL in the medial thalamus is a primary receiving area for somatosensory input, presumably affective and motivational aspects of pain processing, and contains MORs [21,22] along with endogenous opioid peptides [9,25]. Stimulation of MORs in the CL hyperpolarized the cell and changed its firing pattern on the postsynaptic membrane [2]. Based on these findings and those in the present study, morphine may act presynaptically or postsynaptically to reduce excitatory synaptic transmission to CL neurons from the terminals of the spinothalamic tract, and could modulate nociceptive transmission projecting to the frontal cortex from the CL.

In the present study, morphine induced a marked decrease in the mEPSC frequency while decreasing the mEPSC amplitude in Hb neurons. In contrast, morphine reduced the mEPSC frequency without changing its amplitude in CL neurons. It has been considered that the mEPSC amplitude depends on several factors, including, but not limited to, the amount of transmitter released, postsynaptic sensitivity, and the driving force for the ions that mediate the synaptic current [35]. Thus, the fact that the mEPSC amplitude was decreased by morphine in the Hb but not the CL seems to result from differences in the MOR distribution: Hb neurons express MORs at high density, whereas CL neurons contain lower levels of MOR. This contention can be supported by the previous finding that morphine decreased the mEPSC amplitude in cultured rat hippocampal

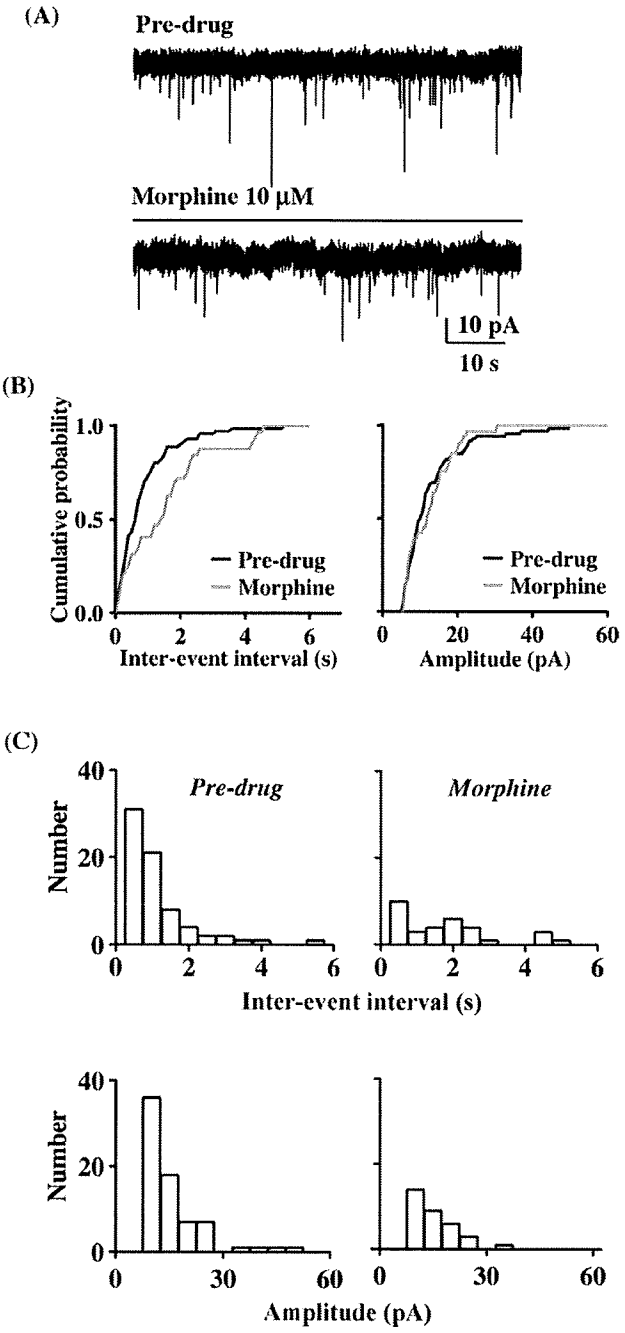

Fig. 2. Presynaptic effect of morphine in the centrolateral thalamic nucleus (CL). (A) Representative mEPSCs recorded in the absence (pre-drug; top) or presence of 10 μM morphine (bottom) at a holding potential of −70 mV. (B) Cumulative distributions of the mEPSC inter-event intervals or amplitude obtained from the same neuron as shown in (A) in the absence (pre-drug) or presence of morphine. (C) Histograms of the number of events per minute plotted against the mEPSC inter-event interval (top) or amplitude (bottom) in the absence (pre-drug; left) or presence of morphine (right). Data were obtained from the same neuron as shown in (A).

neurons overexpressing MORs, whereas it had no effect on intact neurons expressing normal levels of MORs [18].

In the present study, we found that the application of morphine caused either suppression or potentiation of the mEPSC amplitude in respective Hb neurons. These results are also consistent with a previous observation of the complex MOR modulation of glutamatergic synaptic transmission: activation of MOR is associated with either a decrease or increase in NMDA currents in individual

nucleus accumbens neurons [24]. We previously demonstrated that the application of morphine to cultured thalamic neurons evoked a potentiation of postsynaptic glutamate receptor-related currents [28]. Several physiological studies have indicated that opioid receptors can elicit excitatory, as well as inhibitory, modulation through protein kinase C (PKC)-dependent signals [7,28,29]. It has been shown that the activation of PKC enhances mEPSC frequency in the hippocampus [4,14,20,30]. Taken together, these findings suggest that the morphine-induced increase in the mEPSC frequency and amplitude in the Hb may be associated with a PKC pathway via G-protein transduction systems.

Recently, we found that the microinjection of morphine into the Hb enhanced the antinociceptive effect induced by intra-Hb injection with glutamate, which was related to the phenomenon that the application of morphine to cultured thalamic neurons evoked a potentiation of postsynaptic glutamate receptor-related currents [28]. Although the exact mechanisms that underlie this facilitation by morphine are still unclear, our present data suggest that morphine can directly modulate postsynaptic Hb neurons that receive glutamatergic input. It has been demonstrated that Hb neurons receive input from the limbic forebrain and pallidum and, in turn, project to numerous midbrain structures related to the descending pain-control pathway [12,13]. Therefore, the stimulation of excitatory synaptic transmission in the Hb by morphine may be involved in activation of the descending antinociceptive pathway.

In conclusion, we have shown that morphine in the Hb promotes both the inhibition and facilitation of excitatory synaptic transmission, whereas morphine only promotes its reduction in the CL. Our data may provide a cellular basis for the synaptic action of morphine at the thalamus level and support a physiological role for opioids as important inhibitors of sensory information processing in the thalamus. Furthermore, the present data add to the growing list of excitatory synaptic transmission that can be directly regulated by morphine.

References

[1] A.L. Benabid, L. Jeaugey, Cells of the rat lateral habenula respond to high-threshold somatosensory inputs, Neurosci. Lett. 96 (1989) 289–294.
[2] J. Brunton, S. Charpak, mu-Opioid peptides inhibit thalamic neurons, J. Neurosci. 18 (1998) 1671–1678.
[3] M.C. Bushnell, G.H. Duncan, Sensory and affective aspects of pain perception: is medial thalamus restricted to emotional issues? Exp. Brain Res. 78 (1989) 415–418.
[4] R.C. Carroll, R.A. Nicoll, R.C. Malenka, Effects of PKA and PKC on miniature excitatory postsynaptic currents in CA1 pyramidal cells, J. Neurophysiol. 80 (1998) 2797–2800.
[5] S.R. Cohen, R. Melzack, Habenular stimulation produces analgesia in the formalin test, Neurosci. Lett. 70 (1986) 165–169.
[6] S.R. Cohen, R. Melzack, The habenula and pain: repeated electrical stimulation produces prolonged analgesia but lesions have no effect on formalin pain or morphine analgesia, Behav. Brain Res. 54 (1993) 171–178.
[7] S.M. Crain, K.F. Shen, Opioids can evoke direct receptor-mediated excitatory effects on sensory neurons, Trends Pharmacol. Sci. 11 (1990) 77–81.
[8] N. Dafny, J.T. Qiao, Habenular neuron responses to noxious input are modified by dorsal raphe stimulation, Neurol. Res. 12 (1990) 117–121.
[9] J.H. Fallon, F.M. Leslie, Distribution of dynorphin and enkephalin peptides in the rat brain, J. Comp. Neurol. 249 (1986) 293–336.
[10] P. Fatt, B. Katz, Spontaneous subthreshold activity at motor nerve endings, J. Physiol. 117 (1952) 109–128.
[11] G.J. Giesler Jr., R.P. Yezierski, K.D. Gerhart, W.D. Willis, Spinothalamic tract neurons that project to medial and/or lateral thalamic nuclei: evidence for a physiologically novel population of spinal cord neurons, J. Neurophysiol. 46 (1981) 1285–1308.
[12] M. Herkenham, W.J. Nauta, Afferent connections of the habenular nuclei in the rat. A horseradish peroxidase study, with a note on the fiber-of-passage problem, J. Comp. Neurol. 173 (1977) 123–146.
[13] M. Herkenham, W.J. Nauta, Efferent connections of the habenular nuclei in the rat, J. Comp. Neurol. 187 (1979) 19–47.
[14] I. Honda, H. Kamiya, H. Yawo, Re-evaluation of phorbol ester-induced potentiation of transmitter release from mossy fibre terminals of the mouse hippocampus, J. Physiol. 529 (2000) 763–776.
[15] Y. Hori, K. Endo, T. Takahashi, Presynaptic inhibitory action of enkephalin on excitatory transmission in superficial dorsal horn of rat spinal cord, J. Physiol. 450 (1992) 673–685.
[16] S. Jeftinija, Enkephalins modulate excitatory synaptic transmission in the superficial dorsal horn by acting at mu-opioid receptor sites, Brain Res. 460 (1988) 260–268.
[17] T. Kohno, E. Kumamoto, H. Higashi, K. Shimoji, M. Yoshimura, Actions of opioids on excitatory and inhibitory transmission in substantia gelatinosa of adult rat spinal cord, J. Physiol. 518 (1999) 803–813.
[18] D. Liao, O.O. Grigoriants, H.H. Loh, P.Y. Law, Agonist-dependent postsynaptic effects of opioids on miniature excitatory postsynaptic currents in cultured hippocampal neurons, J. Neurophysiol. 97 (2007) 1485–1494.
[19] G. Mahieux, A.L. Benabid, Naloxone-reversible analgesia induced by electrical stimulation of the habenula in the rat, Brain Res. 406 (1987) 118–129.
[20] R.C. Malenka, D.V. Madison, R.A. Nicoll, Potentiation of synaptic transmission in the hippocampus by phorbol esters, Nature 321 (1986) 175–177.
[21] A. Mansour, C.A. Fox, S. Burke, H. Akil, S.J. Watson, Immunohistochemical localization of the cloned mu opioid receptor in the rat CNS, J. Chem. Neuroanat. 8 (1995) 283–305.
[22] A. Mansour, C.A. Fox, S. Burke, F. Meng, R.C. Thompson, H. Akil, S.J. Watson, Mu, delta, and kappa opioid receptor mRNA expression in the rat CNS: an in situ hybridization study, J. Comp. Neurol. 350 (1994) 412–438.
[23] A. Mansour, H. Khachaturian, M.E. Lewis, H. Akil, S.J. Watson, Autoradiographic differentiation of mu, delta, and kappa opioid receptors in the rat forebrain and midbrain, J. Neurosci. 7 (1987) 2445–2464.
[24] G. Martin, Z. Nie, G.R. Siggins, mu-Opioid receptors modulate NMDA receptor-mediated responses in nucleus accumbens neurons, J. Neurosci. 17 (1997) 11–22.
[25] I. Merchenthaler, J.L. Maderdrut, R.A. Altschuler, P. Petrusz, Immunocytochemical localization of proenkephalin-derived peptides in the central nervous system of the rat, Neuroscience 17 (1986) 325–348.
[26] M. Nagao, H. Kamo, I. Akiguchi, J. Kimura, Induction of c-Fos-like protein in the lateral habenular nucleus by persistent noxious peripheral stimulation, Neurosci. Lett. 151 (1993) 37–40.
[27] H. Nakahama, K. Shima, K. Aya, K. Kisara, S. Sakurada, Antinociceptive action of morphine and pentazocine on unit activity in the nucleus centralis lateralis, nucleus ventralis lateralis and nearby structures of the cat, Pain 10 (1981) 47–56.
[28] M. Narita, K. Hashimoto, T. Amano, M. Narita, K. Niikura, A. Nakamura, T. Suzuki, Post-synaptic action of morphine on glutamatergic neuronal transmission related to the descending antinociceptive pathway in the rat thalamus, J. Neurochem. 104 (2008) 469–478.
[29] M. Narita, M. Ohsawa, H. Mizoguchi, T. Aoki, T. Suzuki, L.F. Tseng, Role of the phosphatidylinositol-specific phospholipase C pathway in delta-opioid receptor-mediated antinociception in the mouse spinal cord, Neuroscience 99 (2000) 327–331.
[30] K.D. Parfitt, D.V. Madison, Phorbol esters enhance synaptic transmission by a presynaptic, calcium-dependent mechanism in rat hippocampus, J. Physiol. 471 (1993) 245–268.
[31] P.C. Rinaldi, R.F. Young, D. Albe-Fessard, J. Chodakiewitz, Spontaneous neuronal hyperactivity in the medial and intralaminar thalamic nuclei of patients with deafferentation pain, J. Neurosurg. 74 (1991) 415–421.
[32] B.C. Shyu, B. Olausson, B. Rydenhag, Field potential analysis of the cortical projection of the central lateral nucleus in the cat, Acta Physiol. Scand. 137 (1989) 503–512.
[33] M.G. Terenzi, F.S. Guimaraes, W.A. Prado, Antinociception induced by stimulation of the habenular complex of the rat, Brain Res. 524 (1990) 213–218.
[34] M.G. Terenzi, W.A. Prado, Antinociception elicited by electrical or chemical stimulation of the rat habenular complex and its sensitivity to systemic antagonists, Brain Res. 535 (1990) 18–24.
[35] W. Van der Kloot, The regulation of quantal size, Prog. Neurobiol. 36 (1991) 93–130.
[36] C.W. Vaughan, M.J. Christie, Presynaptic inhibitory action of opioids on synaptic transmission in the rat periaqueductal grey in vitro, J. Physiol. 498 (1997) 463–472.
[37] B.A. Vogt, S. Derbyshire, A.K. Jones, Pain processing in four regions of human cingulate cortex localized with co-registered PET and MR imaging, Eur. J. Neurosci. 8 (1996) 1461–1473.

Neuroscience Letters 453 (2009) 62–67

Contents lists available at ScienceDirect

Neuroscience Letters

journal homepage: www.elsevier.com/locate/neulet

μ-Opioid receptor-independent fashion of the suppression of sodium currents by μ-opioid analgesics in thalamic neurons

Keisuke Hashimoto[a], Taku Amano[a,b], Akiko Kasakura[a], George R. Uhl[c], Ichiro Sora[d], Norio Sakai[b], Naoko Kuzumaki[a], Tsutomu Suzuki[a,*], Minoru Narita[a,*]

[a] Department of Toxicology, Hoshi University School of Pharmacy and Pharmaceutical Sciences, 2-4-41 Ebara, Shinagawa-ku, Tokyo 142-8501, Japan
[b] Department of Molecular and Pharmacological Neuroscience, Division of Integrated Medical Science, Graduate School of Biomedical Sciences, Hiroshima University, 1-2-3 Kasumi, Minami-ku, Hiroshima 734-8551, Japan
[c] Molecular Neurobiology, National Institute on Drug Abuse, Intramural Research Program, TRIAD Bldg., Suite 3501, 333 Cassell Drive, Baltimore, MD 21224, United States
[d] Department of Biological Psychiatry, Tohoku University Graduate School of Medicine, 1-1 Seiryo-machi, Sendai 980-8574, Japan

ARTICLE INFO

Article history:
Received 16 January 2009
Accepted 27 January 2009

Keywords:
Morphine
Fentanyl
Oxycodone
Lidocaine
Voltage-gated sodium channels

ABSTRACT

Most reports in the literature have shown that the effects of opioid analgesics are primarily mediated by μ-opioid receptor (MOR), whereas other potential targets of opioid analgesics have not been thoroughly characterized. In this study, we found that extracellular application of morphine, fentanyl or oxycodone, which are all considered to be MOR agonists, at relatively high concentrations, but not endogenous μ-opioid peptides, produced a concentration-dependent suppression of sodium currents in cultured thalamic neurons. These effects of opioids were not affected by either a MOR antagonist naloxone or a deletion of MOR gene. Among these opioids, fentanyl strongly suppressed sodium currents to the same degree as lidocaine, and both morphine and oxycodone slightly but significantly reduced sodium currents when they were present extracellularly. In contrast, the intracellular application of morphine, but not oxycodone, fentanyl or lidocaine, reduced sodium currents. These results suggest that morphine, fentanyl and oxycodone each produce the MOR-independent suppression of sodium currents by distinct mechanisms in thalamic neurons.

μ-Opioid receptor (MOR) is the principle physiological target for most clinically important opioid analgesics, including morphine, fentanyl and oxycodone [9,12]. It is well known that opioid receptors transduce signals through pertussis toxin-sensitive G_i/G_o proteins to inhibit adenylyl cyclase, increase membrane K^+ conductance and reduce Ca^{2+} current, which leads to cell hyperpolarization and exerts an inhibitory effect [3,4,14]. Several physiological studies have also demonstrated that opioid receptors can activate phospholipase C/protein kinase C-linked pathways [15] in a diverse range of opioid-modulated events, such as pain regulation [11,13] and the response to neuronal excitability [11]. Although there are interesting pharmacological differences in the analgesic potency and the frequency and intensity of adverse events among opioid analgesics classified as MOR agonists, the potential targets of opioid analgesics other than MOR have not been thoroughly characterized.

There is broad agreement on the general outlines of the afferent transmission pathways from primary afferent nociceptors through the dorsal horn to the thalamus. Although the thalamus constitutes the main gateway through which the cerebral cortex receives external sensory signals, there have been relatively few studies on the mechanism of the analgesic effect of opioid analgesics on the thalamus.

Voltage-gated sodium channels play an important role in excitable cells such as nerve and muscle cells. Sodium channels generate rapid and transient inward currents that permit neuronal firing and axonal conduction. Sodium channels are also the target of several classes of drugs, including anesthetics, analgesics, antiepileptics, antidepressants and antiarrhythmics. Therefore, in this study we investigated whether clinically used opioid analgesics could affect voltage-gated sodium channels in rat thalamic neurons, and examined the mechanism by which they affect this channel.

The present study was conducted in accordance with the Guiding Principles for the Care and Use of Laboratory Animals (Hoshi University), as adopted by the Committee on Animal Research of Hoshi University, which is accredited by the Ministry of Education, Culture, Sports, Science, and Technology of Japan. Thalamic neuron/glia co-cultures were grown as follows. The thalamic region was obtained from Sprague–Dawley rat (Tokyo Laboratory Animals Science, Tokyo, Japan) embryos on embryonic day 17 or $MOR^{-/-}$ mice [16] at postnatal 1 day, minced, and treated with papain (9 U/ml, Worthington Biochemical, Lakewood, NJ, USA). After being

* Corresponding authors. Tel./fax: +81 3 5498 5831 (T. Suzuki); Tel.: +81 3 5498 5628 (M. Narita).
E-mail addresses: suzuki@hoshi.ac.jp (T. Suzuki), narita@hoshi.ac.jp (M. Narita).

0304-3940/$ – see front matter © 2009 Elsevier Ireland Ltd. All rights reserved.
doi:10.1016/j.neulet.2009.01.066

treated with enzyme at 37 °C for 15 min, cells were seeded on poly-L-lysine-coated coverslips at a density of 2×10^6 cells/cm^3. The cells were maintained for 10–14 days in Dulbecco's modified Eagle's medium (Invitrogen, Grand Island, NY, USA) supplemented with 10% precolostrum newborn calf serum (Invitrogen), 10 U/ml penicillin and 10 μg/ml streptomycin. Standard whole-cell voltage-clamp recordings were made from cultured thalamic neurons at room temperature using an Axopatch 200B amplifier (Axon Instruments, Foster City, CA, USA). To selectively record sodium currents, the pipette solution contained: 115 CsCl, 25 NaCl, 2 $MgCl_2$, 1 $CaCl_2$, 11 EGTA and 10 HEPES, pH 7.4 with CsOH. The external bath solution contained the following (in mM): 100 NaCl, 40 tetraethylammonium-Cl, 0.03 $CaCl_2$, 10 HEPES, 10 $MgCl_2$, 10 D-glucose, pH 7.4 with TEA-OH. The patch microelectrodes were made from borosilicate capillary glass and had resistances of 5–10 MΩ for the whole-cell recording. Under voltage-clamp recording conditions, the series resistance was 4–7 MΩ. Leak currents were subtracted by a P/4 pulse protocol except for the experiments on use-dependent block, and the series resistance was compensated by 70–80% in all experiments. The signals filtered at 2 kHz were directly digitized and stored on a personal computer. These sampled measurements were analyzed using the pCLAMP8 program (Axon Instruments). In repeated tests, voltage steps of 20 ms duration were applied every 20 s from a resting potential of −70 mV to a test potential of −20 mV. Availability protocols consisted of a series of prepulses between −100 mV and −20 mV in 10-mV increments lasting 1 s, from a holding potential of −70 mV, followed by a 20-ms depolarization to −20 mV. The normalized curves were fitted using a Boltzmann distribution equation: $I/I_{max} = 1/(1 + \exp((V_m - V_{1/2})/k))$, where I_{max} is the peak sodium current elicited after the most hyperpolarized prepulse, V_m is the preconditioning pulse potential, $V_{1/2}$ is the potential at which inactivation is half-maximal, and k is the slope factor. Unless otherwise noted, statistical analyses were performed using Student's t-test. The opioid analgesics used in the present study were morphine hydrochloride (Daiichi–Sankyo Co., Tokyo, Japan), fentanyl citrate (a kind gift from Hisamitsu Pharmaceutical Co. Inc., Tokyo, Japan) and oxycodone hydrochloride (a kind gift from Shionogi Pharmaceutical Co. Inc., Osaka, Japan). Lidocaine, naloxone, β-endorphin, endomorphin-1, endomorphin-2 and QX-314 were obtained from Sigma–Aldrich (St. Louis, MO, USA).

To determine if morphine, fentanyl and oxycodone could affect voltage-dependent sodium currents, whole-cell sodium currents were recorded in rat cultured thalamic neurons. Each opioid analgesic and the sodium channel blocker lidocaine reduced sodium currents in a concentration-dependent manner in rat cultured thalamic neurons (Fig. 1B). The IC_{50} values for morphine, fentanyl, oxycodone and lidocaine were 1053 μM (920–1206 μM), 153.2 μM (132.7–170.2 μM), 1260 μM (1135–1398 μM) and 350.2 μM (303.0–404.6 μM), respectively. The suppression of sodium currents was observed immediately after bath application of 100 μM morphine, fentanyl and oxycodone, and these inhibitions were reversible on washing (Supplementary Fig. 1). Under these recording conditions, tetrodotoxin blocked all channel currents (data not shown). In acute thalamic slices, sodium currents were suppressed by 100 μM morphine (Supplementary Fig. 2). To determine whether MOR contributes to the reduction of sodium currents by opioid analgesics, we first tested the effects of the opioid receptor antagonist naloxone on the suppression of sodium currents by opioid analgesics in cultured thalamic neurons. Bath application of 10 μM naloxone failed to block the inhibitory effects of 100 μM morphine (16.5 ± 3.3%; morphine + naloxone, 15.5 ± 3.1%, $n = 7$), fentanyl (35.9 ± 0.6%; fentanyl + naloxone, 35.6 ± 4.8%, $n = 3$) and oxycodone (12.6 ± 1.2%; oxycodone + naloxone, 14.9 ± 1.6%, $n = 4$) (Fig. 1C). Furthermore, to confirm the MOR-independent fashion of the fentanyl-induced suppression of sodium currents, we used thalamic neurons obtained from $MOR^{-/-}$ mice. After the bath application of 100 μM fentanyl, sodium currents were clearly suppressed in thalamic neurons with no detectable MORs ($I/I_0 = 0.659 \pm 0.033$, $p < 0.001$, $n = 5$, Fig. 1D). We next tested whether endogenous μ-opioid peptides could affect the sodium currents in rat cultured thalamic neurons. Application of β-endorphin, endomorphin-1 or endomorphin-2 (1, 10 or 100 μM) did not affect the amplitude of sodium current (100 μM; decrease by 4.0 ± 1.5%, 2.7 ± 0.5%, −1.1 ± 2.9%, respectively, Fig. 1E).

A common property of local anesthetics used clinically is that they preferentially affect the channel at a specific stage in its cycle of rest, activation and inactivation, often by delaying recovery from the inactivated state, thereby producing a cumulative reduction of sodium currents called 'use-dependent' block [5]. In the present study, the suppression of sodium currents by 100 μM fentanyl or lidocaine was use-dependent, as demonstrated by a progressive decrease in current during repetitive stimulation from −100 mV to −20 mV at 10 Hz (Fig. 2A and D). After the bath application of 100 μM fentanyl or lidocaine, the ratio of current amplitude was decreased at the first pulse (34.7 ± 2.1%, $n = 5$, or 13.6 ± 6.6%, $n = 4$, respectively), and at the 10th pulse (55.2 ± 1.9% or 31.0 ± 4.6%, respectively), compared with before drugs (Fig. 2B and E). A further analysis of the pulse-by-pulse decrease revealed that the suppression of sodium current by fentanyl or lidocaine was use-dependent (first pulse versus 10th pulse; 31.5 ± 1.6% or 29.0 ± 7.9%, respectively, Fig. 2C and F).

Local anesthetics can produce hyperpolarizing shifts in steady-state inactivation by binding to a receptor site on the ion channel [1,7]. In the present study, the application of 100 μM morphine (−4.8 ± 1.1 mV, $n = 7$), fentanyl (−8.6 ± 0.9 mV, $n = 7$), oxycodone (−3.6 ± 0.4 mV, $n = 4$) and lidocaine (−9.3 ± 0.6 mV, $n = 3$) caused hyperpolarizing shifts in $V_{1/2}$ of steady-state inactivation (Fig. 2G–J).

Most local anesthetics used clinically are relatively hydrophobic molecules that gain access to their blocking site on the sodium channel by diffusing into or through the cell membrane [7]. To determine the apparent sidedness of drug action, we measured the sodium currents elicited by a depolarizing step pulse (from −70 mV to −20 mV, 20 ms) in cells filled with each opioid analgesic or lidocaine. QX-314, a positively charged derivative of lidocaine, has no effect on neuronal sodium channels when applied extracellularly, but blocks sodium channels when applied intracellularly [2,6,17]. Consistent with this finding, QX-314 (10 mM) totally suppressed sodium current in our experiments (Fig. 3A and B). The addition of oxycodone, fentanyl or lidocaine at 10 mM to the recording pipette had no effect on sodium currents compared with a control pipette solution (peak amplitude = −3099.4 ± 140.4 pA with oxycodone, $n = 4$, −2850.5 ± 572.8 pA with fentanyl, $n = 5$, −2522.4 ± 569.6 pA with lidocaine, $n = 4$, Fig. 3A and B), whereas the sodium current was almost totally abolished by bath application of these drugs at the same concentration (Fig. 1B). On the other hand, the addition of 10 mM morphine to the recording pipette significantly reduced sodium currents (peak amplitude = −897.7 ± 119.0 pA, $p < 0.001$, $n = 6$, Fig. 3A and B). We also asked whether the intracellular application of fentanyl or lidocaine could affect the suppression of sodium currents caused by the extracellular application of fentanyl or lidocaine. In the presence of intracellular fentanyl or lidocaine at 10 mM, extracellular application of 100 μM fentanyl or lidocaine caused current suppression (39.7 ± 0.2% or 26.0 ± 0.2%, respectively, Fig. 3C). Furthermore, this was observed at approximately the same level as in the absence of intracellular fentanyl or lidocaine (37.0 ± 2.0% or 22.9 ± 1.8%, respectively, Fig. 3C).

It has been well established that opioid analgesics inhibit cAMP formation, close voltage-sensitive Ca^{2+} channels and open K^+ channels though MOR, which leads to cell hyperpolarization and exerts an inhibitory effect [3,4,14]. In this study, we used whole-cell voltage-clamp recording and found that, as with lidocaine, extra-

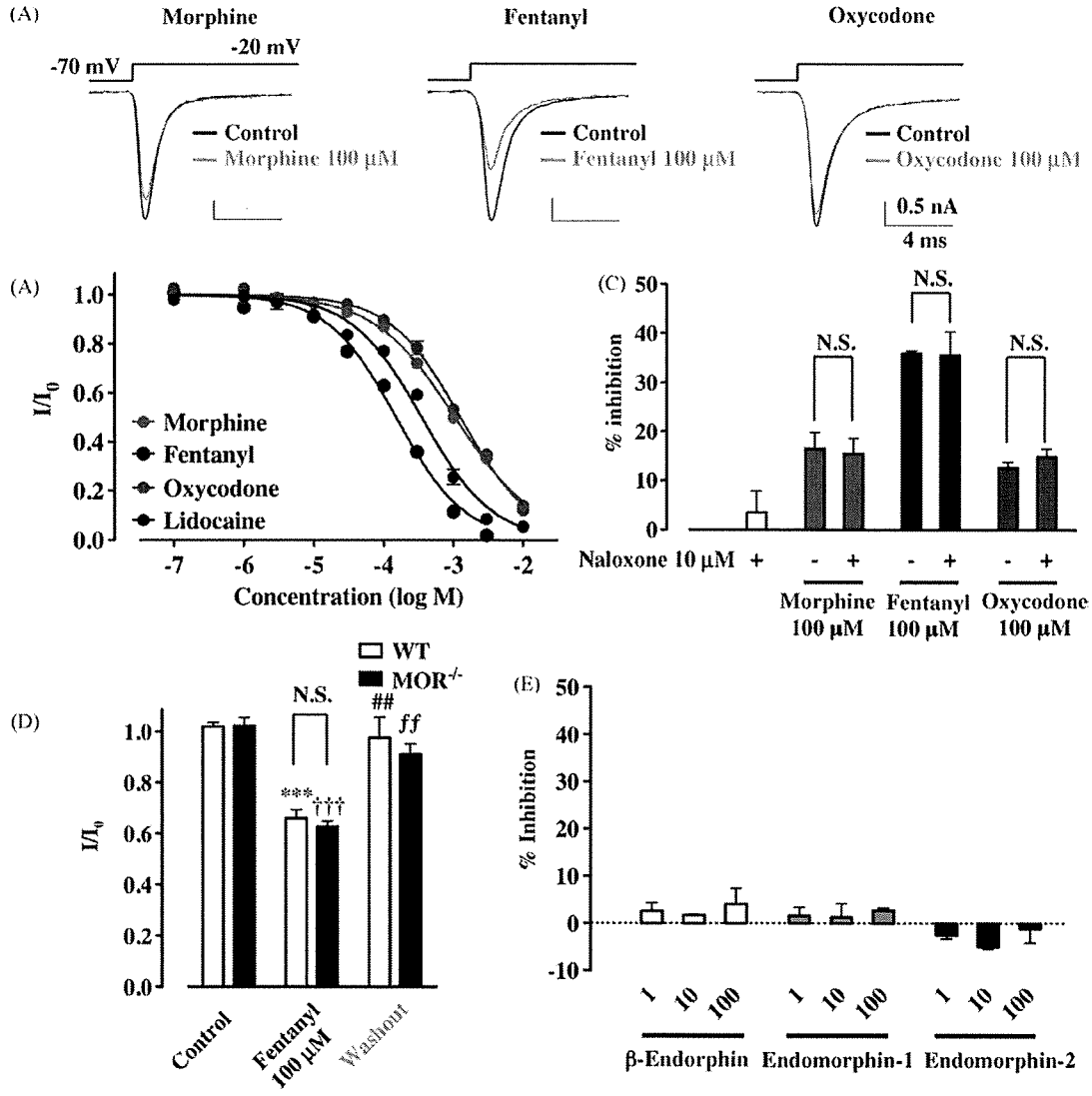

Fig. 1. Suppression of sodium currents by opioid analgesics in rat thalamic neuron through non-opioidergic mechanisms. Voltage steps were applied from a holding potential of −70 mV to a test potential of −20 mV. (A) Representative current traces obtained in the presence or absence of 100 μM morphine, fentanyl or oxycodone. (B) Concentration-dependent inhibition of the sodium currents by morphine, fentanyl, oxycodone and lidocaine in rat cultured thalamic neurons. Each symbol represents the mean value of normalized peak currents in the presence of drug (I/I_0, mean ± S.E.M.), derived from 3 to 8 independent experiments for each concentration tested. (C) No effects of the opioid receptor antagonist naloxone (10 μM) on suppression of sodium currents by the bath application of 100 μM morphine, fentanyl or oxycodone. (D) No involvement of MORs in fentanyl-induced suppression of sodium currents in thalamic neurons using $MOR^{-/-}$ mice. Each column represents the normalized peak current amplitudes (I/I_0, mean ± S.E.M., $n = 5$). $^{***}p < 0.001$ control (WT) vs. fentanyl (WT), $^{\#\#}p < 0.01$ fentanyl (WT) vs. washout (WT), $^{\dagger\dagger\dagger}p < 0.001$ control ($MOR^{-/-}$) vs. fentanyl ($MOR^{-/-}$), $^{ff}p < 0.01$ fentanyl ($MOR^{-/-}$) vs. washout ($MOR^{-/-}$). (E) Effects of endogenous μ-opioid peptides on voltage-gated sodium channels in rat cultured thalamic neurons. No significant changes in sodium currents were observed with the bath application of 1–100 μM β-endorphin ($n = 5$–7), endomorphin-1 ($n = 3$) or endomorphin-2 ($n = 3$–8). Each column represents the mean value of the %inhibition of the peak amplitude of the sodium currents in the presence of drug (mean ± S.E.M.).

cellular application of morphine, fentanyl or oxycodone produced a concentration-dependent suppression of sodium currents, which was not influenced by the opioid receptor antagonist naloxone. In agreement with these findings, the effect of fentanyl on sodium current suppression was clearly shown in thalamic neurons obtained from $MOR^{-/-}$ mice. Moreover, endogenous μ-opioid peptides did not affect the amplitude of sodium currents. These findings clearly indicate that morphine, fentanyl and oxycodone suppress thalamic sodium currents through non-opioidergic mechanisms.

We also found that, among these opioids, the inhibitory potency of the extracellular application of fentanyl was much stronger than those of the other two opioids, to the same degree as lidocaine. Although further study is required, the similarity of the chemical structures of fentanyl and lidocaine may help to explain the similarity of their potencies, as well as the difference in the sodium channel-blocking effects of fentanyl, morphine or oxycodone. There is a broad consensus that most local anesthetics used clinically gain access to their blocking site on the sodium channel by diffusing into or through the cell membrane [7]. In addition, the site at which local anesthetics act, at least in their charged form, is accessible only from the inner surface of the membrane [10]. Lidocaine, morphine, oxycodone and fentanyl have pK_a values of 7.8, 7.9, 8.5 and 8.4, respectively, which means that more than 80% of the drug is ionized at physiological pH. Even though large amounts of lidocaine, fentanyl and oxycodone are ionized at experimental pH, the present data clearly show that the internal application of fentanyl, oxycodone or lidocaine failed to suppress sodium currents, whereas external application of the same drugs suppressed sodium currents

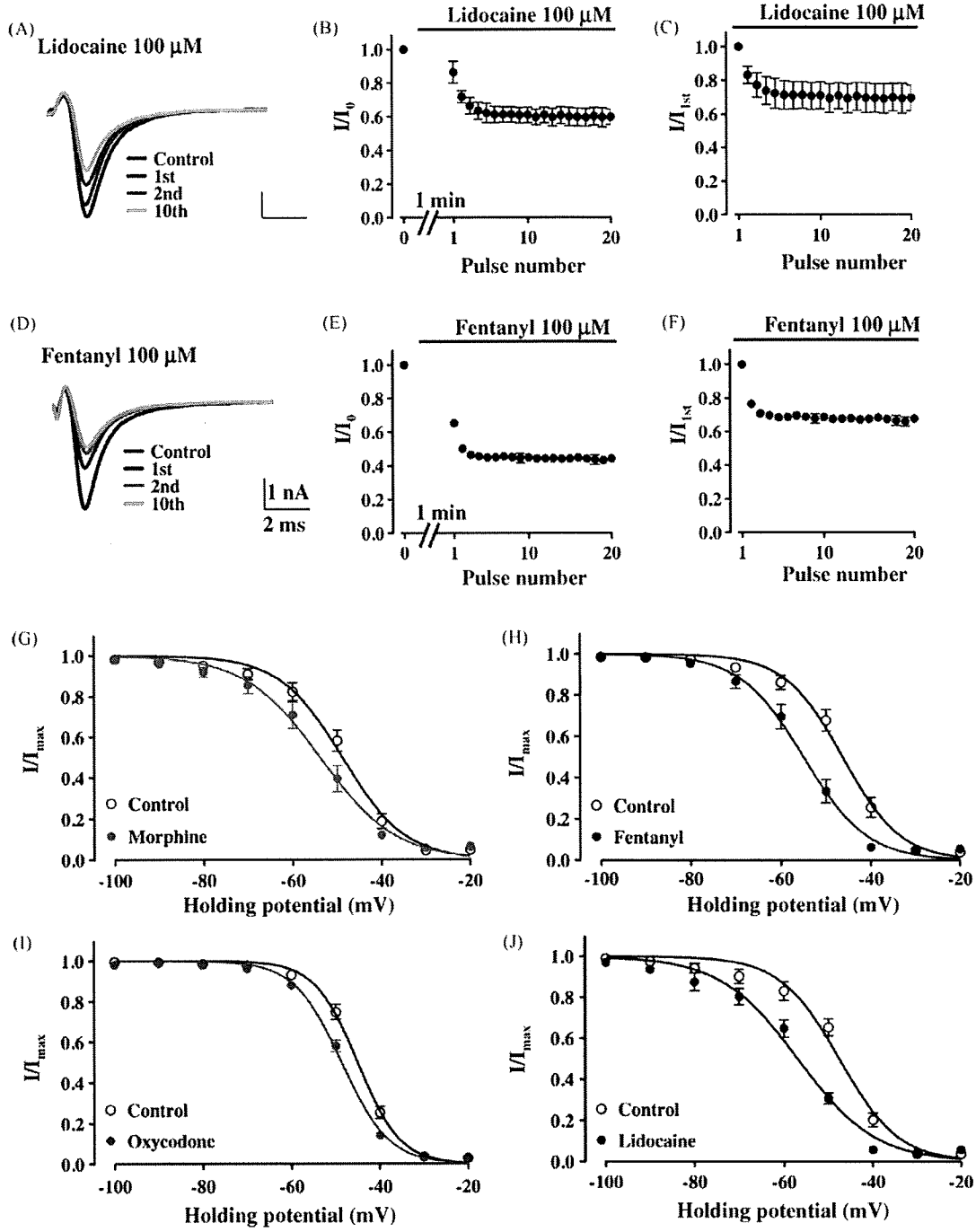

Fig. 2. A common feature of the effects of opioid analgesics and local anesthetics on sodium current suppression. (A–F) Use-dependent block of sodium currents by lidocaine and fentanyl. Use-dependent block was examined at 10 Hz with 30 20-ms test pulses to −20 mV from a holding potential of −100 mV. Repeated test potentials were given 1 min after the bath application of 100 μM lidocaine or fentanyl. (A and D) Representative traces show currents elicited by the pre-drug (Control) and first (1st), second (2nd) or 10th pulses after the bath application of lidocaine or fentanyl. (B, C, E, F) Time-course changes in use-dependent block. Peak current amplitudes were normalized to the control peak current amplitude (I/I_0, mean ± S.E.M., B and E) or to the initial peak current amplitude in the presence of drug (I/I_{1st}, mean ± S.E.M., C and F) and plotted against the pulse number. (G–J) Voltage-dependence of inactivation for the sodium current in rat cultured thalamic neurons. The voltage-dependence of channel inactivation in the absence (Control) and presence of 100 μM morphine (G), fentanyl (H), oxycodone (I) or lidocaine (J) was estimated by measuring the peak amplitude of the sodium current during a test potential (−20 mV) from a variable holding potential. The current at each membrane potential was divided by the electrochemical driving force for sodium ions and normalized to the maximum sodium current (I_{max}).

with different potencies. Furthermore, in the presence of intracellular fentanyl or lidocaine, extracellular application of fentanyl or lidocaine, respectively, caused current suppression to approximately the same level as that in the absence of intracellular fentanyl or lidocaine. This phenomenon induced by lidocaine is consistent with a recent report that external, but not internal, application of the sodium channel blocker flecainide promotes use-dependent block of heart sodium channels [8]. Thus, the present data strongly suggest that either fentanyl- or lidocaine-induced sodium current suppression may occur when drugs are present extracellularly. In

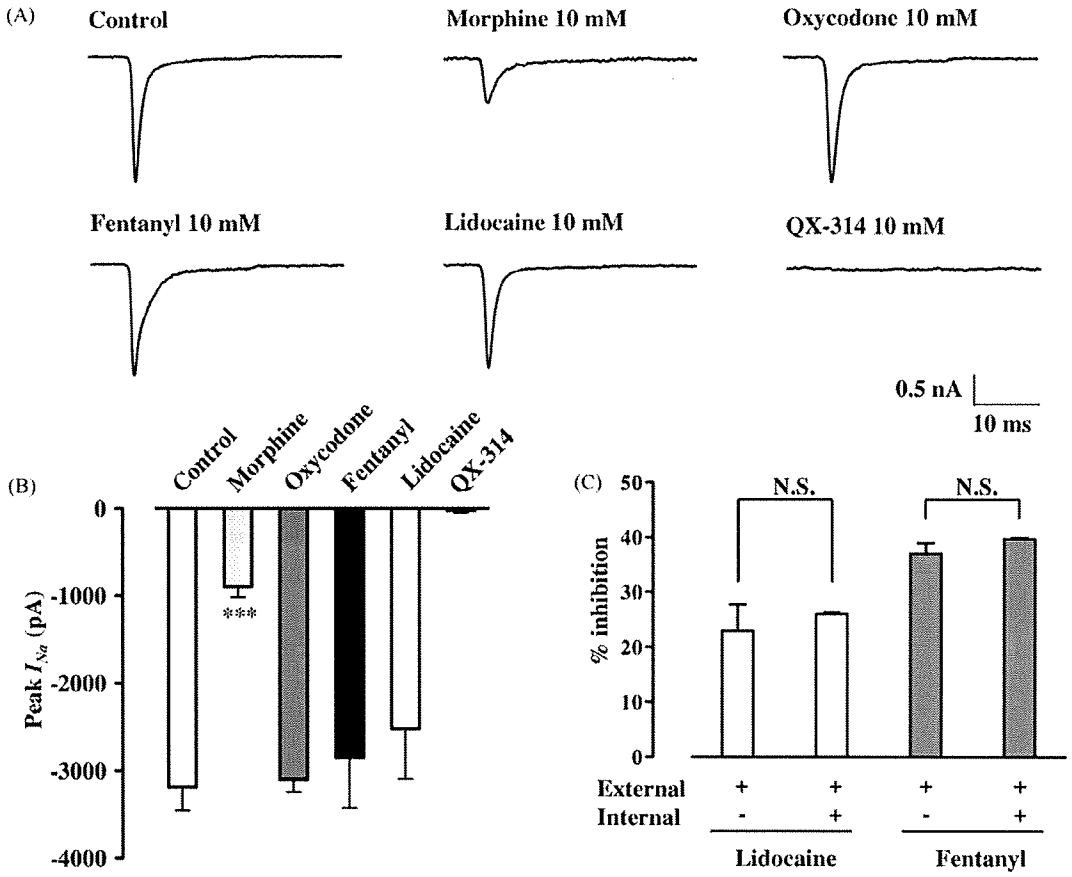

Fig. 3. The effect of intracellular application of opioid analgesics in whole-cell configurations. (A) Representative traces show the currents in a control pipette solution and in the presence of intracellular morphine (10 mM), oxycodone (10 mM), fentanyl (10 mM), lidocaine (10 mM) and the lidocaine derivative QX-314 (10 mM). Currents were elicited by 20-ms depolarizing steps from a holding potential of −70 mV to a test potential of −20 mV. Pulses were applied until steady-state sodium currents were achieved. (B) Bar graphs summarize steady-state sodium currents with the internal application of morphine, oxycodone, fentanyl, lidocaine and QX-314. Each column represents the mean value of the peak currents with S.E.M. $^{***}p < 0.001$ vs. control. (C) Test of sidedness of fentanyl block using whole-cell recordings. Suppression of sodium currents by the extracellular application of 100 μM lidocaine or fentanyl was measured in the absence or presence of intracellular lidocaine (10 mM) or fentanyl (10 mM). Each column represents the mean value of the %inhibition of the peak amplitude of the sodium currents in the presence of drugs (mean ± S.E.M.).

contrast, morphine caused a significant suppression of sodium currents when applied either internally or externally, but with different potencies. These findings suggest that, like lidocaine, either fentanyl or oxycodone may have a blocking effect on sodium currents by acting through the extracellular pathway, whereas morphine may act through both the extracellular and intracellular pathway.

Use-dependent block, where the inhibitory effect on channels by a drug cumulatively increases with repetitive stimulation at high frequency, which mostly indicates that the drug can block the channel current when the channel is activated (open), is the hallmark for local anesthetics. In the present study, depending on the pulse number, both lidocaine and fentanyl progressively decreased the peak amplitude of sodium currents at a holding potential of −100 mV, indicating that fentanyl effectively blocks the sodium channel current when the channel gate is open. We also found that fentanyl, but not lidocaine, caused the tonic suppression of sodium currents with no depolarizing stimulation at a holding potential of −100 mV, and that almost all thalamic sodium channels were maintained with a resting state. These findings suggest that the inhibition of sodium channels by fentanyl may result from its multiple effects on sodium channels in both the resting and activated (channel open) states.

It has been reported that a local anesthetic binds more tightly to and stabilizes the inactivated state of the sodium channel [1,5,7]. Consistent with these observations with local anesthetics, we demonstrated that lidocaine showed hyperpolarizing shifts in the steady-state inactivation of voltage-gated sodium channels. Under the present conditions, we found that the extracellular application of these three opioids gave the same performance as with exposure to lidocaine. The present data suggest that, like lidocaine, morphine, fentanyl and oxycodone suppress sodium currents by facilitating inactivation of a thalamic sodium channel at a normal resting membrane potential when these three opioids are applied extracellularly.

In conclusion, we have shown that opioid analgesics in thalamic neurons may promote the inhibition of neuronal activity by blocking voltage-gated sodium channels without MOR activation. Furthermore, our data suggest that three MOR agonists exhibit different blocking potencies toward sodium channels with distinct mechanisms. In future studies, it might be worthwhile to ascertain whether these opioid analgesics directly access their binding domains on voltage-gated sodium channels and how to facilitate their blocking effects.

Appendix A. Supplementary data

Supplementary data associated with this article can be found, in the online version, at doi:10.1016/j.neulet.2009.01.066.

References

[1] B.P. Bean, C.J. Cohen, R.W. Tsien, Lidocaine block of cardiac sodium channels, J. Gen. Physiol. 81 (1983) 613–642.
[2] M.D. Cahalan, W. Almers, Interactions between quaternary lidocaine, the sodium channel gates, and tetrodotoxin, Biophys. J. 27 (1979) 39–55.
[3] S.R. Childers, Opioid receptor-coupled second messenger systems, Life Sci. 48 (1991) 1991–2003.
[4] M.J. Christie, R.A. North, Agonists at mu-opioid, M2-muscarinic and GABAB-receptors increase the same potassium conductance in rat lateral parabrachial neurones, Br. J. Pharmacol. 95 (1988) 896–902.
[5] K.R. Courtney, Mechanism of frequency-dependent inhibition of sodium currents in frog myelinated nerve by the lidocaine derivative GEA, J. Pharmacol. Exp. Ther. 195 (1975) 225–236.
[6] D.T. Frazier, T. Narahashi, M. Yamada, The site of action and active form of local anesthetics. II. Experiments with quaternary compounds, J. Pharmacol. Exp. Ther. 171 (1970) 45–51.
[7] B. Hille, Local anesthetics: hydrophilic and hydrophobic pathways for the drug-receptor reaction, J. Gen. Physiol. 69 (1977) 497–515.
[8] H. Liu, J. Atkins, R.S. Kass, Common molecular determinants of flecainide and lidocaine block of heart Na+ channels: evidence from experiments with neutral and quaternary flecainide analogues, J. Gen. Physiol. 121 (2003) 199–214.
[9] H. Mizoguchi, H.E. Wu, M. Narita, I. Sora, S.F. Hall, G.R. Uhl, H.H. Loh, H. Nagase, L.F. Tseng, Lack of mu-opioid receptor-mediated G-protein activation in the spinal cord of mice lacking Exon 1 or Exons 2 and 3 of the MOR-1 gene, J. Pharmacol. Sci. 93 (2003) 423–429.
[10] T. Narahashi, D.T. Frazier, Site of action and active form of local anesthetics, Neurosci. Res. 4 (1971) 65–99.
[11] M. Narita, K. Hashimoto, T. Amano, M. Narita, K. Niikura, A. Nakamura, T. Suzuki, Post-synaptic action of morphine on glutamatergic neuronal transmission related to the descending antinociceptive pathway in the rat thalamus, J. Neurochem. 104 (2008) 469–478.
[12] M. Narita, A. Nakamura, M. Ozaki, S. Imai, K. Miyoshi, M. Suzuki, T. Suzuki, Comparative pharmacological profiles of morphine and oxycodone under a neuropathic pain-like state in mice: evidence for less sensitivity to morphine, Neuropsychopharmacology 33 (2008) 1097–1112.
[13] M. Narita, M. Ohsawa, H. Mizoguchi, T. Aoki, T. Suzuki, L.F. Tseng, Role of the phosphatidylinositol-specific phospholipase C pathway in delta-opioid receptor-mediated antinociception in the mouse spinal cord, Neuroscience 99 (2000) 327–331.
[14] H. Rhim, R.J. Miller, Opioid receptors modulate diverse types of calcium channels in the nucleus tractus solitarius of the rat, J. Neurosci. 14 (1994) 7608–7615.
[15] D. Smart, G. Smith, D.G. Lambert, Mu-opioids activate phospholipase C in SH-SY5Y human neuroblastoma cells via calcium-channel opening, Biochem. J. 305 (1995) 577–581.
[16] I. Sora, N. Takahashi, M. Funada, H. Ujike, R.S. Revay, D.M. Donovan, L.L. Miner, G.R. Uhl, Opiate receptor knockout mice define mu receptor roles in endogenous nociceptive responses and morphine-induced analgesia, Proc. Natl. Acad. Sci. U.S.A. 94 (1997) 1544–1549.
[17] G.R. Strichartz, The inhibition of sodium currents in myelinated nerve by quaternary derivatives of lidocaine, J. Gen. Physiol. 62 (1973) 37–57.

Bioorganic & Medicinal Chemistry Letters 19 (2009) 438–441

Contents lists available at ScienceDirect

Bioorganic & Medicinal Chemistry Letters

journal homepage: www.elsevier.com/locate/bmcl

Synthesis of novel twin drug consisting of 8-oxaendoethanotetrahydromorphides with a 1,4-dioxane spacer and its pharmacological activities: μ, κ, and putative ε opioid receptor antagonists

Hideaki Fujii [a], Akio Watanabe [a], Toru Nemoto [a], Minoru Narita [b], Kan Miyoshi [b], Atsushi Nakamura [b], Tsutomu Suzuki [b], Hiroshi Nagase [a,*]

[a] Department of Medicinal Chemistry, School of Pharmacy, Kitasato University 5-9-1, Shirokane, Minato-ku, Tokyo 108-8641, Japan
[b] Department of Toxicology, Hoshi University, School of Pharmacy and Pharmaceutical Sciences 2-4-41, Ebara, Shinagawa-ku, Tokyo 142-8501, Japan

ARTICLE INFO

Article history:
Received 17 October 2008
Revised 11 November 2008
Accepted 13 November 2008
Available online 18 November 2008

Keywords:
Opioid
Twin drug
Monomer
ε-Antagonist

ABSTRACT

A twin drug consisting of 8-oxaendoethanotetrahydromorphides with a 1,4-dioxane spacer, NS29, was synthesized from a naltrexone derivative. The structure of compound **8**, the precursor of NS29, was determined by X-ray crystallography. Monomeric NS28 showed μ opioid receptor antagonist activity, whereas dimeric NS29, consisting of two NS28 units, showed antagonist activities for μ, κ, and the putative ε opioid receptor agonists. Twin drug NS29 and its derivatives are expected to be unique pharmacological tools for investigation of opioid receptor types

Opioid receptors are generally classified into μ, δ, and κ types not only by pharmacological studies but also by molecular biological characterizations, and all receptor types are related to analgesic effect.[1] Based on the detailed investigation of pharmacological effects using selective ligands, each receptor type has been further divided into subtypes (μ_1, μ_2, δ_1, δ_2, κ_1, κ_2, and κ_3).[1] In addition to these three types, a putative ε opioid receptor was proposed as the receptor specifically binding the endogenous opioid peptide, β-endorphin, based on various pharmacological observations.[2] Although the three types of the opioid receptors (μ, δ, and κ) have been cloned, the opioid receptor subtypes and the putative ε opioid receptor have not yet. On the other hand, the dimerization of a variety of G-protein-coupled receptors (GPCRs) has been reported and the homo- or hetero-dimerization of GPCRs could modulate their pharmacological effects.[3] The opioid receptor is also known to form homo- and hetero-dimers.[3,4] A recent proposal has attributed the diversity of the opioid pharmacological effects to the dimerization of the corresponding receptor types, an idea which differs from the earlier concept that opioid receptor subtypes (perhaps including the putative ε receptor)[5] are responsible for the heterogeneous effects.

We have already synthesized ε-agonist TAN-821[6] and ε-antagonist TAN-1014 (Fig. 1).[7] Although these ligands showed selectivity for the putative ε opioid receptor in the mouse tail-flick and hot-plate assays, the selectivity was not sufficient in the binding assay. To obtain a more selective ligand for the putative ε opioid receptor, we designed and synthesized the 8-oxaendoethanotetrahydromorphide derivatives (Fig. 1) on the basis of the following working hypothesis: (1) the strong affinities of TAN-821 and TAN-1014 for the opioid receptors stemmed from their high lipophilicity,

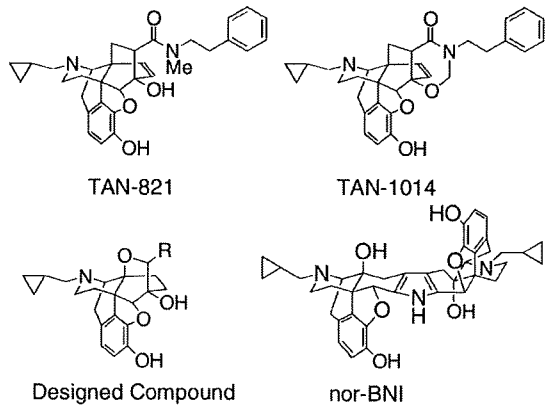

Figure 1. Structures of TAN-821, TAN-1014, designed compound, and nor-BNI.

* Corresponding author. Tel.: +81 3 5791 6372; fax: +81 3 3442 5707.
E-mail address: nagaseh@pharm.kitasato-u.ac.jp (H. Nagase).

0960-894X/$ - see front matter © 2008 Elsevier Ltd. All rights reserved.
doi:10.1016/j.bmcl.2008.11.050

which may cause their low selectivity in vitro; (2) the introduction of a hydrophilic moiety into the basic bicyclo[2.2.2]octane skeleton of these ligands could decrease its lipophilicity.[8] In the course of our attempts to synthesize the designed compound, a novel twin drug with a 1,4-dioxane spacer was obtained unexpectedly. In general, a twin drug, dimeric ligand is one of the most useful tools for the investigation of pharmacological properties of some receptors and enzymes because a dimeric ligand can induce unique effects which a monomeric structure never shows.[9] An identical twin drug consisting of two identical pharmacophoric entities could increase the binding affinity and/or efficacy compared with that of the corresponding monomeric ligand, while a non-identical twin drug bearing two different pharmacophoric entities is expected to bind to the respective receptors for each monomeric ligand and could elicit the corresponding effects derived from the individual receptors.[8] Furthermore, a twin drug can sometimes show an unexpected effect, which may not be predicted from each monomeric unit. For example, nor-BNI (Fig. 1), consisting of two identical units of the μ opioid receptor antagonist naltrexone with a pyrrole spacer, showed selective κ opioid receptor antagonist activity.[10] Herein, we report synthesis of the novel twin drug NS29 and describe its pharmacological effects.

An acetal exchange reaction of dithiane **1** derived from naltrexone methyl ether **10** with $HC(OMe)_3$ and $CuCl_2/CuO$ afforded orthoester **2** predominantly (Scheme 1).[8] On the other hand, the acetal exchange reaction of **1** with $HC(OMe)_3$ and $CuCl_2$ in the presence of camphorsulfonic acid (CSA) provided a mixture of acyclic acetal **3** and cyclic acetal **4** instead of the orthoester **2** (Scheme 1). Hydrolysis of the mixture of acetals **3** and **4** gave an inseparable mixture of α-hydroxyl aldehyde **5**, its hemiacetal dimer **7**, and cyclic hemiacetal **6**. As the α-hydroxy aldehyde is known to be prone to transform into five and six membered dimers,[11] we attempted to lead the mixture of compounds **5**, **6**, and **7** toward the acetal dimer **8**. After extensive investigations, we found that treatment of the mixture of compounds **5**, **6**, and **7** with CSA under azeotropic distillation provided the objective dimer **8**. Compound **8** was chemically stable and subsequently converted to dimer **9** (NS29) by demethylation. The structure of compound **8**, confirmed by X-ray crystallography (Fig. 2), consisted of two 8-oxa-endoethanotetrahydromorphide skeletons with a 1,4-dioxane spacer.[12] For comparison with the pharmacological profile of dimer **9**, compound **13** (NS28), which corresponded to the monomeric component of dimer **9**, was also synthesized from naltrexone methyl ether **10** in two steps according to a reported method (Scheme 2).[13]

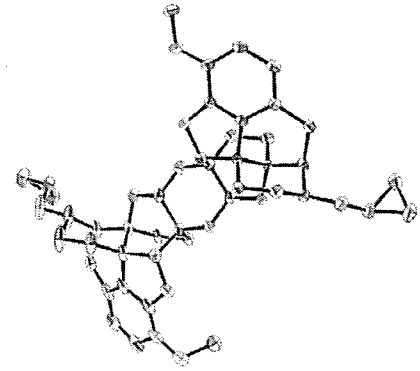

Figure 2. X-ray crystallography of compound **8**. Crystal water in the crystal structure was omitted for clarity.

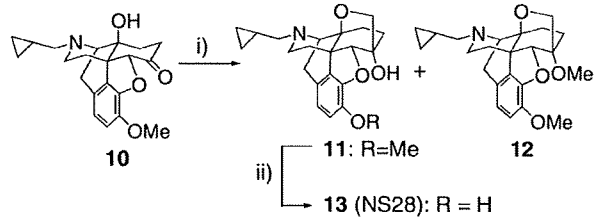

Scheme 2. (i) NaH, $Me_3S^+I^-$, THF, DMSO, rt, 62% for **11**, 26% for **12**; (ii) *t*-BuOK, *n*-PrSH, DMF, 150 °C, 96%.

The effects of NS29 and NS28 on G-protein activation introduced by selective opioid agonists were evaluated by [^{35}S]GTPγS binding to mouse whole brain without cerebellum membranes (μ, δ, and putative ε receptors) or to the guinea pig cerebellum (κ receptor). NS29 blocked the stimulation of [^{35}S]GTPγS binding induced by μ-agonist morphine (10^{-5} M), κ-agonist U50,488H (10^{-5} M), and putative ε-agonist β-endorphin[14] (10^{-6} M) (Fig. 3(A), (C), and (D), respectively) in a concentration-dependent manner. However, the stimulation of [^{35}S]GTPγS binding induced by δ-agonist SNC-80 (10^{-5} M) was not affected by NS29 (Fig. 3(B)). These results indicated that NS29 may be an antagonist against the μ-, κ-, and putative ε-receptors. Antagonist activity of NS29 for β-endorphin was strong, but weaker for morphine and U50,488H. On the other hand, NS28 inhibited the stimulation of

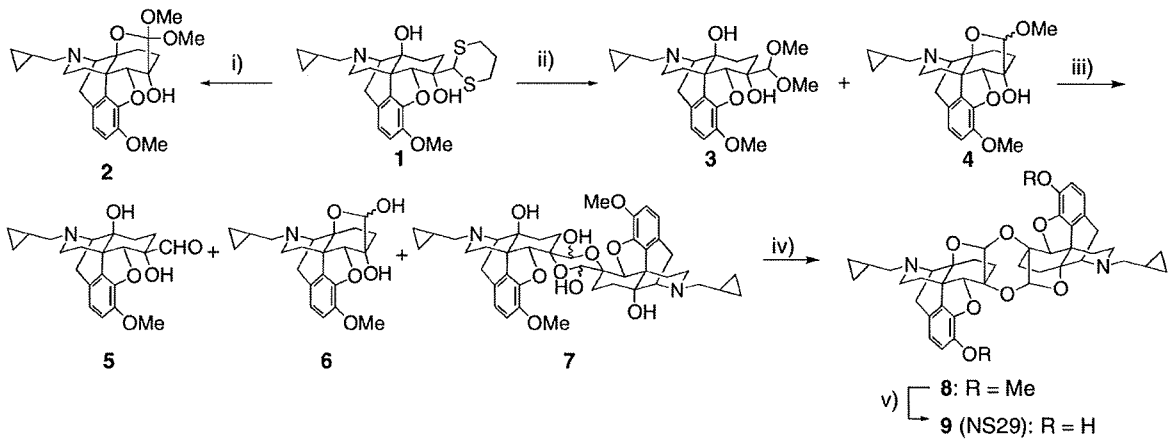

Scheme 1. Reagents and conditions: (i) $CH(OMe)_3$, $CuCl_2/CuO$, MeOH, 50 °C, 78%; (ii) $CH(OMe)_3$, $CuCl_2$/CSA, MeOH, 50 °C, 9 h, 65% for **3**, 18% for **4**; (iii) 1 M HCl, reflux; (iv) CSA, toluene, reflux, 23%; (v) *t*-BuOK, *n*-PrSH, DMF, 150 °C, 82%.

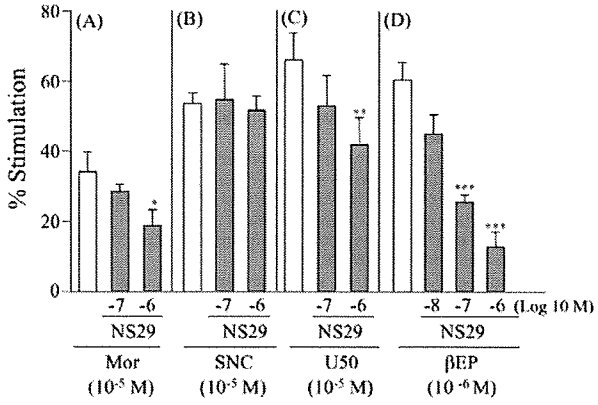

Figure 3. Effects of NS29 on G-protein activation induced by μ (A), δ (B), κ (C), and putative ε (D) opioid receptor agonist.

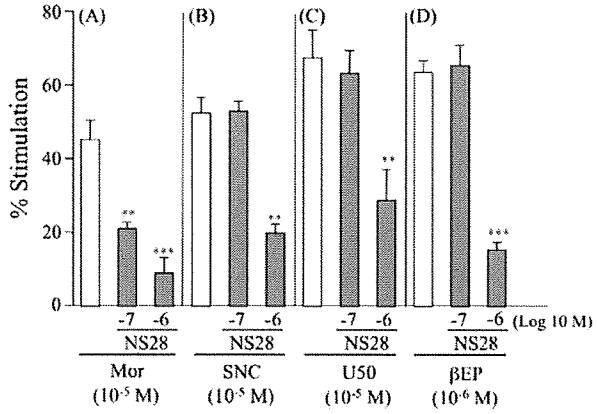

Figure 4. Effects of NS28 on G-protein activation induced by μ (A), δ (B), κ (C), and putative ε (D) opioid receptor agonist.

[^{35}S]GTPγS binding induced by μ-agonist morphine (10^{-5} M) concentration-dependently (Fig. 4(A)). However, the stimulation of [^{35}S]GTPγS binding induced by δ-agonist SNC-80 (10^{-5} M), κ-agonist U50,488H (10^{-5} M), and putative ε-agonist β-endorphin (10^{-6} M) was blocked by only the highest concentration of NS28 (10^{-6} M), but the effect was not concentration dependent (Fig. 4(B), (C), and (D)). These results suggested that NS28 would be a μ-antagonist.

The monomeric NS28 showed μ-antagonist activity, while dimeric NS29 exhibited strong antagonism for putative ε opioid receptors and weak antagonism for μ and κ opioid receptor in the [^{35}S]GTPγS binding assay. The results indicated that the dimerization of NS28 into the twin drug NS29 afforded an additional pharmacological effect, a strong putative ε-antagonist activity. In the opioid field, the 'message–address concept' is a well-known means to characterize ligands that are specific for different receptor types,[15] and several selective ligands have been designed and synthesized on the basis of this concept.[16] According to the concept, selective opioid ligands can be divided into two parts, the message-site and the address-site. The former site could be the necessary structure to produce the opioid intrinsic effects while the latter site could participate in the receptor type selectivity. Figure 5 illustrates the individual message sites and the address sites in putative ε-agonist TAN-821 and in NS29. Previously, we developed a working hypothesis for the selective binding of TAN-821 with the putative ε receptor: the address site for the putative ε receptor would be located above the C ring of 4,5-epoxymorphinan skeleton.[6] The 7α-carboxamide side chain in TAN-821 would

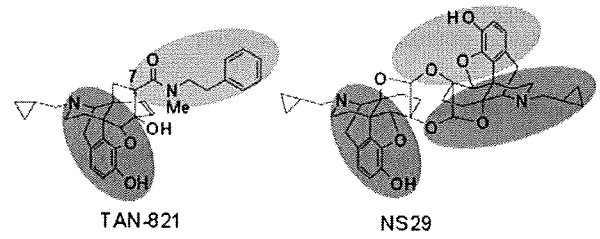

Figure 5. Message, address, and possible accessory site of TAN-821 and NS29 are indicated by blue, green, and red circles, respectively.

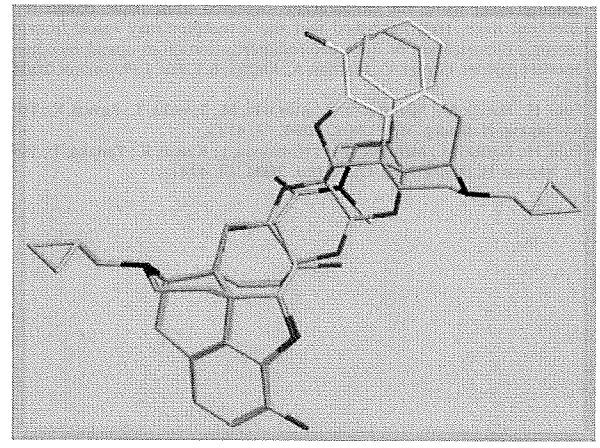

Figure 6. Superimposition of the 3D-aligment of TAN-821 onto that of NS29. Notable benzene rings, and nitrogen and oxygen atoms are indicated by yellow, blue, and red color, respectively.

act as the address site (Fig. 5). Particularly, the phenyl group in the address site was deduced to play an important role in binding to the putative ε receptor.

Each benzene ring of TAN-821 and NS29 in the address site (indicated by yellow color in Fig. 6) appears to occupy a similar location when the 3D-alignment of TAN-821 was superimposed onto that of NS29 (Fig. 6). The benzene ring shown at the upper right side in NS29 may act as the address site for the putative ε receptor. Moreover, NS29 has a bulkier lipophilic structure than TAN-821. Antagonists generally possess bulky, lipophilic moieties, the so-called accessory site,[17] which could interfere with the conformational change in the receptor which is required to induce agonistic activity. The bulky lipophilic moiety of NS29 indicated by a red circle in Figure 5 could function as an accessory site.

A twin drug such as NS29 may clarify whether various pharmacological effects of opioids derive from opioid receptor subtypes or whether they can be to the result of the dimerization of the corresponding receptor types, especially δ–κ and μ–δ heterodimers.

In conclusion, identical twin drug NS29, consisting of two NS28 molecules linked by a 1,4-dioxane spacer, was synthesized from naltrexone methyl ether, whose structure was determined by X-ray crystallography. NS29 attenuated the [^{35}S]GTPγS binding induced by μ-, κ-, or the putative ε-agonist, while NS28 blocked only the μ-agonist induced [^{35}S]GTPγS binding. Dimer NS29 and its derivatives are expected to be unique pharmacological tools for the investigation of opioid receptors.

Acknowledgments

We acknowledge the financial supports from Shorai Foundation for Science and the Uehara Memorial Foundation. We also